SPECTRAL PROPERTIES OF FRACTAL LATTICES

by

Alain Douchant

A thesis
presented to the University of Manitoba
in partial fulfillment of the
requirements for the degree of
M.Sc.
in
Physics

Winnipeg, Manitoba

SPECTRAL PROPERTIES OF FRACTAL LATTICES

BY

ALAIN ROBERT DOUCHANT

A thesis submitted to the Faculty of Graduate Studies of the University of Manitoba in partial fulfillment of the requirements of the degree of

MASTER OF SCIENCE

ABSTRACT

The spectral properties of a d- dimensional bond percolating network have been examined using a real-space rescaling approach. Both the triangular and face-centered cubic lattices have been studied where the disorder has been modelled with the d- dimensional Sierpinski gasket. The vibrational density of states $\rho(\omega^2)$ and the integrated density of states $N(\omega^2)$ have been calculated using functional integral methods. The spectra of these systems have been calculated as a function of concentration p and are characterized by an infinite number of energy bands as well as a large number of localized modes as the percolation threshold Pc is approached from above. We find that two excitation regimes exist that are characterized by two separate dimensions: one for length scales above the correlation length ξ which is the Euclidean dimension d and one for length scales below ξ known as the spectral dimension. The specific heat has been calculated and the low temperature behaviour examined. A crossover in the behaviour at low temperature as a function of p-Pc has been observed. Our results could be important for understanding the physical properties of quasi-crystalline materials.

ACKNOWLEDGEMENTS

I would like to give special thanks to Dr. Southern whose expertise, guidance and patience made this project an enjoyable experience for me. I would like to extend my appreciation to Dr. Loly for his help and useful comments and I would also like to thank the graduate students in the theory group (a great bunch) in particular Javid Ashraff whose help was beneficial and greatly appreciated. Finally, thanks to Rhonda Roman for her care and moral support during the course of my thesis.

TABLE OF CONTENTS

1 INTRODUCTION

1.1 DISORDERED SYSTEMS

Thermodynamic and physical properties of solids are closely associated with the dynamics of the constituent particles and in particular with the nature of the distribution of the frequencies of these degrees of freedom. This information about the spectral properties is obtained by first solving the time-independent Schrödinger equation for a single particle

$$H\psi(\vec{r})=E\psi(\vec{r}) \qquad [1.1]$$

where H is the Hamiltonian operator and $\psi(\vec{r})$ is the wavefunction. The success of 'solid state physics' in understanding the properties of crystalline materials is due to the fact that crystals possess translational invariance and hence so do the solutions to the Schrödinger equation. The eigenfunctions $\psi(\vec{r})$ of the Hamiltonian H are known as Bloch functions (Bloch, 1928) and can be written in the form

$$\psi(n,\vec{k};\vec{r})=\exp[i(\vec{k}.\vec{r})]u(n,\vec{k};\vec{r}) \qquad [1.2]$$

where $u(n,\vec{k};\vec{r})$ has the periodicity of the crystal lattice and $\vec{k}$ is a wavevector in the first Brillouin zone of the reciprocal lattice. The probability for a particle described by $|\psi(\vec{r})|^2$ to be at a given point is the same for all equivalent points in the lattice. The quantum number "n" is known as an energy band index which takes on integer values and labels the various allowed values of the energy at each value of $\vec{k}$. These energy eigenvalues $E(n;\vec{k})$ take the form of continuous bands of energy separated by gaps and are referred to as the band structure of the crystal. This information can be used to calculate the electrical, mechanical and thermal properties of pure crystalline materials using the quantum mechanical distribution functions (see for example Ashcroft and Mermin (1976)).

The success of quantum mechanics in explaining the spectral properties of crystalline materials led to the application of these same ideas to non-crystalline materials or disordered solids. Various types of disorder are shown in figure 1.1 and fall into the following three general classes (see for example Ziman (1979a) and Rickayzen(1980)):

1. Substitutional disorder: Atoms of a pure lattice are replaced at random by atoms of a different type.
2. Structural disorder: The original lattice is distorted but there exists a one-one correspondence between sites of the disordered lattice and those sites of the original lattice.

Figure 1.1: Different types of disorder; (a) is substitutional, (b) is structural, (c) is topological (Rickayzen 1980).

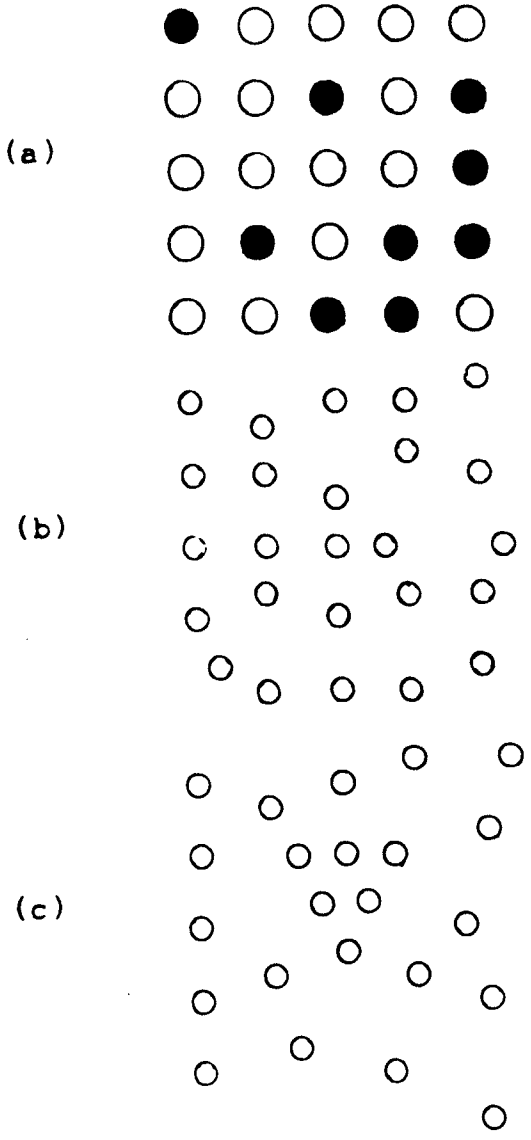

3. Topological disorder: The original lattice is distorted but there is no longer a one-one correspondence as in the preceding class.

In each of these cases, translational invariance is destroyed . Hence a major difficulty associated with the study of disordered systems is that we cannot use many of the familiar concepts derived from the study of crystalline materials. Concepts such as Bloch's theorem cannot be used to simplify the mathematical procedure required to solve the Schrödinger equation.

Theoretical studies of such complex systems are often carried out using simple model systems . A complete analytical treatment of real systems would otherwise be an impossible task with the exception of some simple disordered cases. For this reason, the theory of excitations in disordered systems is often discussed in terms of a standard mathematical model referred to as the "tight binding model".

The tight-binding model or the tight-binding Hamiltonian (TBH) is defined as follows (Economou, 1983):

$$H=\sum_i |i\rangle \epsilon(i) \langle i| + \sum_{i\neq j} |i\rangle V(i,j) \langle j| \qquad [1.3]$$

where $\{|i>\}$ are atomic-like orbitals centered at each site "i". The parameter $\epsilon(i)$ represents the energy of a particle trapped at the site i and $V(i,j)$ is a parameter describing the extent to which a particle can "hop" from a site "i" to a site "j". The spectral properties of systems described by the TBH are conveniently studied within a Green's function formalism.

The Green's functions are solutions of the following matrix equation

$$(z-H)G=I \qquad [1.4]$$

where I is the identity matrix,z is a complex energy and H is the Hamiltonian.The matrix elements of G are given by

$$G(i,j)=<i|(z-H)^{-1}|j> \qquad [1.5]$$

Since the eigenvalues of H are real, $G(i,j)$ is an analytic function in the complex z-plane except at points or regions on the real axis which correspond to these eigenvalues .

The local density of states is obtained from the diagonal elements $G(i,i)$ in the limit as the imaginary part of $z=E+is$ approaches zero.

$$\rho(i;E)=-(1/\pi)\lim_{s\to 0}\{\mathrm{Im}G(i,i)\} \qquad [1.6]$$

The average density of states per site is thus

$$\rho(E)=(1/N)[\sum_{i}\rho(i;E)] \qquad [1.7]$$

and represents the fraction of eigenstates in the energy interval (E,E+dE). Another quantity of interest is the cumulated or integrated density of states which represents the total number of states up to energy E and is defined as follows

$$N(E)=\int\rho(\lambda)d\lambda \qquad [1.8]$$

where the limits of integration are from $-\infty$ to E.

For the tight-binding Hamiltonian in equation [1.3], the Green's functions are solutions of the following set of equations

$$[z-\epsilon(i)]G(i,j)=\delta(i,j) + \sum_{k}V(i,k)G(k,j) \qquad [1.9]$$

where $\delta(i,j)$ is the Kronecker delta. In this standard form, the equations are frequently used to study the electronic, vibrational and magnetic excitations in solids.

The differences between ordered and disordered systems are apparent when we calculate the Green's function and the corresponding the density of states for both types of systems. In the perfectly ordered case, the wave functions are the extended Bloch states with continuous bands of allowed energies separated by gaps. The density of states for these translationally invariant systems are generally smooth functions of energy. However, disordered systems are much more complex. Extended states are replaced by wavefunctions that are limited to a finite coherence length. When disorder is introduced in a crystalline material it can give rise to localized energy levels outside the normal band of the perfect crystal. Energy gaps will exist between those localized levels and the normal band and if the amount of disorder is increased further, then so will the number of localized levels . Moreover, the wavefunctions of these levels may eventually overlap each other or with the normal band. The spectral structure then no longer simply consists only of continuous energy bands but rather of a collection of both continuous bands and jagged peaks and for this reason it is not possible to carry out analytical treatments of such systems. Figure 1.2 shows the computed frequency spectra of disordered chains by Dean (1961,1972)

Numerical approaches which perform computer simulation of these models are a more feasible way of obtaining the properties of disordered systems. The numerical methods

Figure 1.2: Computed squared frequency spectra for disordered chains of length 8000 atoms of mass ratio 3:1 with equal nearest neighbour force constants and different concentrations, c, of light atoms (Dean, 1972).

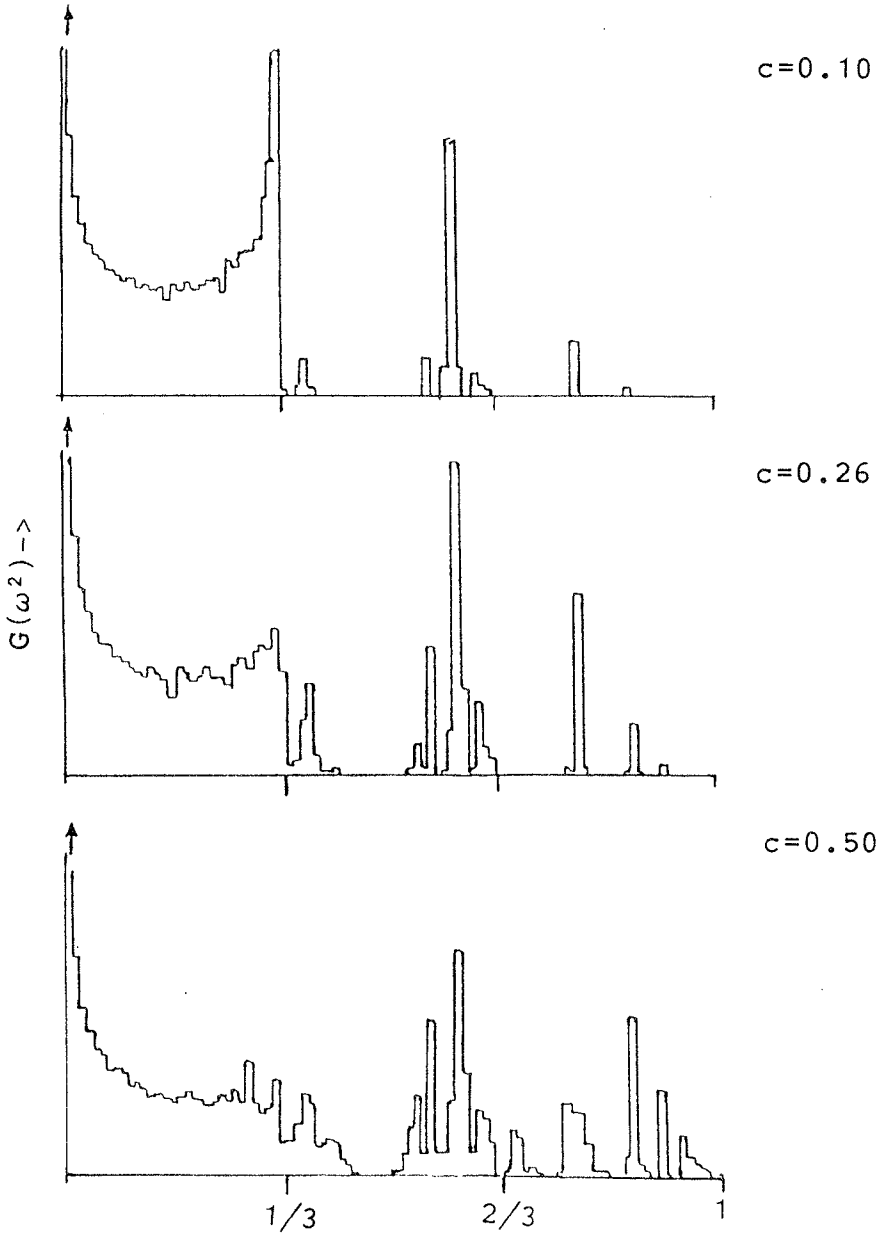

currently employed are varied and each is useful in its own way. One of the desired goals is to make such methods "efficient" in terms of algorithm and computer time. The Recursion (or Lanczos) method (Haydock, 1980), for instance, involves taking the Hamiltonian of a physical system and transforming it into a symmetric three term recursion relation. In such a procedure, a set of orthonormal orbitals and a corresponding set of recurrence parameters are calculated recursively. These quantities are represented graphically by a pseudo chain where the nodes of the chain represent the orbitals and the connection between the nodes represent the recurrence parameters. The spectral properties of the system are then obtained by calculating the Green's function which is written in terms of a continued fraction using the parameters of the chain model.

Another method is based on the Renormalization Group approach (Wilson, 1971a,b). The idea behind renormalization is to take a system on a large scale and to reduce it to a smaller more manageable size. This approach is appropriate if the physics of the system that one is considering involves fluctuations over widely different scales of length. For instance, a Hamiltonian describes the interactions between particles in a lattice at lengths comparable to the lattice spacing. To determine the bulk properties for the lattice using the Hamiltonian requires a summation over all sites in the system but this would be

impractical if the number of particles that we are dealing with is of the order of 10^{23} . Instead, we divide the system into smaller more manageable groups. Each group consisting of a comparatively small number of interacting particles is reduced for example to one particle with new effective interactions. The particles remaining from each group are separated by larger distances but all lengths are renormalized so that the original scale that we had at the beginning is restored. This technique was originally used in the study of critical phenomena, but can also be used to evaluate the spectral properties of ordered and disordered systems. Such ideas are incorporated into the rescaling method (Southern et al, 1983a; Southern et al, 1983b; Southern and Loly, 1984).

Rescaling involves taking a Hamiltonian, such as the TBH, which describes a system with N degrees of freedom and "reducing" it in the sense that we eliminate a fraction of the sites in a progressive manner. At each stage,this process reduces the number of degrees of freedom and is also known as decimation. The system is then renormalized, that is, all lengths are rescaled to obtain the original structure of the system before sites were eliminated. The matrix elements of the TBH are also renormalized so that it is in a form similar to the original TBH matrix. This procedure is then repeated indefinitely until one degree of freedom is left and the resulting elements are then used to determine the Green's function.

1.2 SCOPE OF THESIS

A model of a disordered system in both two and three dimensions is introduced and the spectral properties are calculated using a rescaling method. In chapter II, we describe the rescaling method in detail using a 1-d TB model as an example and compare the spectral properties obtained from such a method with a Fourier Transform approach. It should be noted that the rescaling method is performed in direct space while the Fourier Transform process makes use of reciprocal space. We also describe what is called the percolation model and show how it is used to model disordered systems. We will show how the concept of fractal dimension arises from studies of this model. Finally, at the end the chapter, we describe a technique for determining the density of states using a generating function approach.

In chapter III, we examine certain disordered systems in two and three dimensions. We will demonstrate how fractal lattices can be used to represent disorder in perfect systems. The perfect lattices that we will be using are the triangular and face centered cubic lattices. The density of states of these disordered systems will be evaluated using the techniques described in chapter II. The specific heat of a disordered lattice network will be calculated and the results compared with the perfect lattice systems.

The final chapter contains a summary and conclusion.

2 SCALING

The conventional method of calculating the density of states per site on a perfect lattice involves the use of Fourier transforms. The convenience in using such transformations in perfect systems is that they immediately "diagonalize" the problem at hand. However, the results that we obtain are in reciprocal or "k" space rather than direct space. When the parameters in the TBH (which is written in direct space) are translationally invariant,we can perform a Fourier Transformation which readily gives the desired energy eigenvalues of the Hamiltonian in k-space.

In a translationally invariant system the parameters in the TBH of equation [1.3] can be written as

$$\epsilon(i)=\epsilon \text{ for all } i \qquad [2.1a]$$

$$V(i,j)=V(|i-j|)=V(l) \qquad [2.1b]$$

The eigenstates have the form (Economou, 1983)

$$|\vec{k}\rangle=(1/\sqrt{N})\sum_{l}\exp(i\vec{k}.\vec{l})\,|\vec{l}\rangle \qquad [2.2]$$

where $|\vec{k})$ is the spatial Fourier Transform of $|1>$. The eigenvalues then are easily shown to be of the form

$$E(k)=\epsilon + \sum_{1} V(1)\exp(i\vec{k}.\vec{1}) \qquad [2.3]$$

The Green's functions from equation [1.5] are immediately given by

$$G(1,m)=\sum_{k}[<\vec{1}|\vec{k})(\vec{k}|\vec{m}>]/[z-E(\vec{k})] \qquad [2.4]$$

This expression is evaluated by summing over k-values in the first Brillouin zone (BZ) so that for any dimension, the matrix elements of G(z) are

$$G(1,m)=[\Omega/(2\pi)^{d}]\int d\vec{k}\{\exp[(i\vec{k}.(\vec{1}-\vec{m})]\}/[z-E(\vec{k})] \qquad [2.5]$$

where "d" denotes the dimensionality of the system and Ω the corresponding volume ($\Omega=L^{d}$). Thus depending on the form of $E(\vec{k})$ for the lattice of interest, the density of states is readily obtained from the diagonal terms in equation [2.5]. The density of states have been evaluated for many lattices such as the linear chain, square and simple cubic lattice (Economou, 1983), for the triangular and honeycomb lattice (Horiguchi, 1972), and for the BCC and FCC lattice (Morita

and Horiguchi, 1970). In most of these cases the V(l) terms in equation [2.3] have been restricted to nearest neighbours only. We can determine the band edges of the energy spectrum by finding the maximum and minimum values of E(k) in the first BZ. For the linear chain,square,simple cubic and BCC lattices,the band edges are at $\epsilon \pm zV$ where z is the number of nearest neighbours of any site in the lattice. For the triangular lattice,the band edges are at $\epsilon-3V$ and $\epsilon+6V$, and for the FCC lattice, the band edges are at $\epsilon-4V$ and $\epsilon+12V$;where V is the nearest neighbour hopping matrix element.

2.1 REAL-SPACE RESCALING

The density of states per site can also be determined using a rescaling method. In what follows, this method is applied in detail to a one-dimensional lattice that is translationally invariant and where we only consider nearest neighbour interactions. For systems with second neighbour interactions, we refer the reader to a paper by Southern et al (1983a). To demonstrate the procedure,we begin with equation [1.9] and since the system is translationally invariant we can use the following simplification

$$G(i,j)=G(|i-j|)=G(l) \qquad [2.6]$$

The complex variable z is written in the form $E+i0^+$ where $i0^+$ is an infinitessimal imaginary number. The lattice Green's functions for nearest neighbour interactions in a linear chain are then obtained from the following equations (i=all integers)

$$(E-\epsilon)G(i)=\delta(i,0) + V[G(i+1)+G(i-1)] \qquad [2.7]$$

We can make the above equation more compact by writing it in terms of reduced variables

$$G(i)=a(i) + x[G(i+1)+G(i-1)] \qquad [2.8]$$

where

$$x=V/(E-\epsilon) \qquad [2.9a]$$

and

$$a(i)=\delta(i,0)/(E-\epsilon) \qquad [2.9b]$$

A given G(i) is coupled to G(i±1) and these lattice functions are determined from

$$G(i\pm1)=a(i\pm1) + x[G(i\pm2)+G(i)] \qquad [2.10]$$

If we identify the index i as even, then equation [2.8] and [2.10] represent equations for the even and odd sites respectively. From these equations, we would like to eliminate certain sites so that we can reduce the number of degrees of freedom in the system. We arbitrarily choose to eliminate the odd sites (or the odd equations) by substituting equation [2.10] for G(i±1) into equation [2.8] to get the following

$$G(i)=a(i) + x\{a(i-1) + x[G(i+2)+G(i)] + [a(i+1) + x[G(i-2)+G(i)]\} \qquad [2.11]$$

Notice that we have eliminated all odd sites and are only left with even sites. Since the indices of G must be even (i=even integer),we can rewrite the above equation in the following equivalent form

$$(1-2x^2)G(2i)=\{a(2i) + x[a(2i-1)+a(2i+1)] + x^2[G(2i+2)+G(2i-2)]\} \qquad [2.12]$$

where i now takes on all integer values. Equation [2.12] has the same form as our original equation [2.8] when written in terms of the following renormalized parameters

$$x'=x^2/(1-2x^2) \qquad [2.13]$$

$$a'(2i)=\{a(2i) + x[a(2i+1)+a(2i-1)]\}/(1-2x^2) \qquad [2.14]$$

Next, the distances between the even sites that remain are rescaled by a factor of two and each site is relabeled as shown in figure 2.1. This means that

$$G(2i) \rightarrow G(i)$$

$$G(2i\pm2) \rightarrow G(i\pm1) \qquad [2.15]$$

and

$$a'(2i) \rightarrow a(i) \qquad [2.16]$$

We can rewrite equation [2.12] as follows:

$$G(i)=a'(i) + x'[G(i+1)+G(i-1)] \qquad [2.17]$$

which has the identical form as equation [2.8] and allows us to repeat the rescaling procedure. To obtain the spectral properties of the one-dimensional uniform lattice (with nearest neighbour interactions), we must only evaluate the local Green's function G(0) since the average Green's function per site is

$$\langle G\rangle=(1/N)\sum_i G(i,i)=G(0) \qquad [2.18]$$

Initially we have $a(0)=1/(E-\epsilon)$ and $a(i)=0$ for $i\neq 0$. The renormalized values $a'(i)$ are all zero except $a'(0)$ which is given by

$$a'(0)=a(0)/(1-2x^2) \qquad [2.19]$$

We can repeat this process of reducing the number of degrees of freedom in the system simply by iterating equations [2.13] and [2.19]. Eventually, after a certain number of iterations (which we denote as k), the parameter x' tends to zero. The $a'(0)$ that remains after k iterations is denoted as $a(\infty;0)$. The local Green's function G(0) is obtained trivially in this limit and is given by

$$G(0)=a(\infty;0) \qquad [2.20]$$

and the density of states is obtained by using equations [1.6] and [1.7]

$$\rho(E)=-(1/\pi)\mathrm{Im}\{G(0)\}= -(1/\pi)a(\infty;0) \qquad [2.21]$$

Figure 2.1: Schematic illustration of the rescaling procedure. The first step consists of "eliminating" the odd sites (dark circles) leaving a chain with only even sites (blank circles). The second step consists of rescaling all lattice distances by a factor of 1/2 and relabeling the sites (from Southern et al, 1983b).

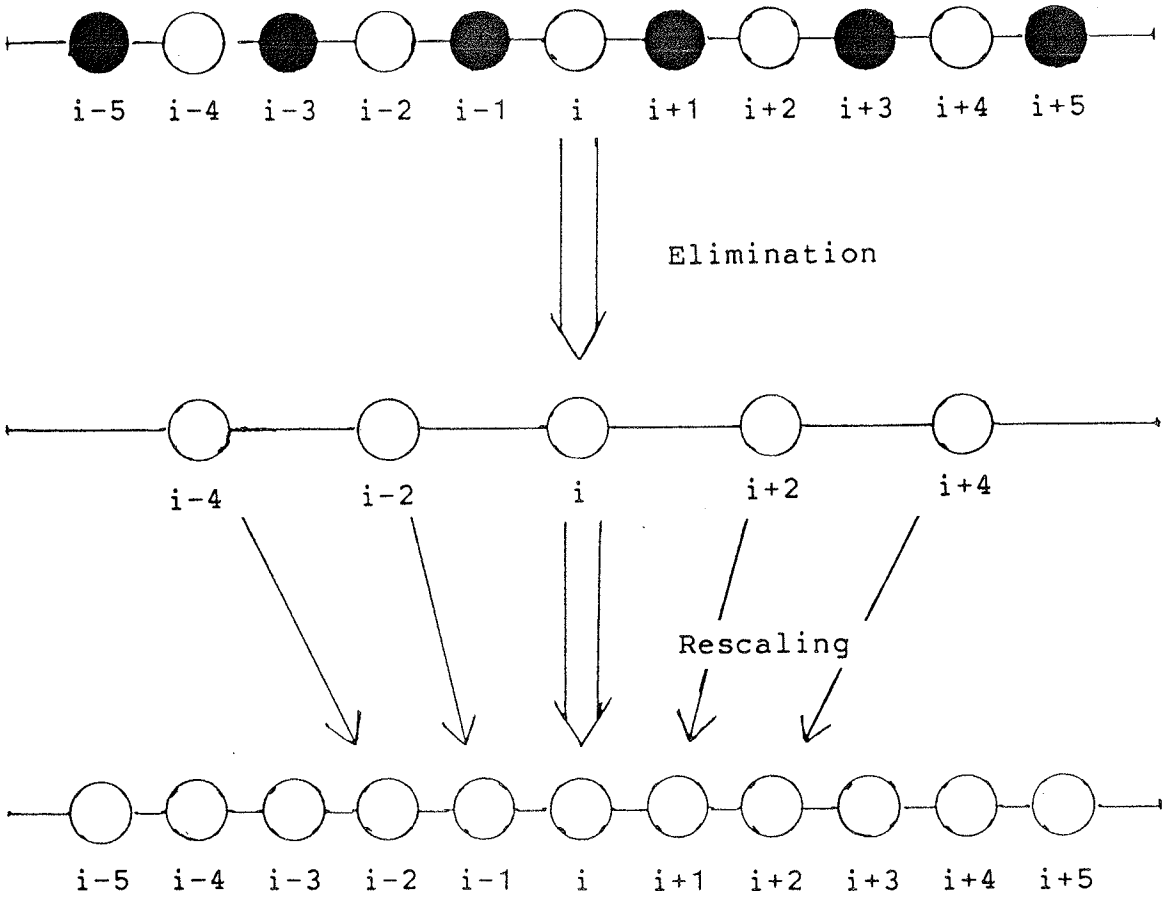

A plot of the Green's function (both real and imaginary part) versus the energy E is shown in figure 2.2. The results obtained for the Green's function using rescaling agree exactly with the Fourier Transform approach for a linear chain (Economou, 1983).

The recurrence relation [2.13] posesses certain "fixed" points, or points where the value of x does not change under iteration (i.e. X=f(X)). It is a non-linear transformation that can be linearized about its fixed points assuming of course that the equation behaves sufficiently smoothly. The fixed points, denoted by X, are obtained by setting x=X in equation [2.13] and solving for X. They are

$$X=-1,\ 0,\ 1/2$$

We now linearize x' about the X's using a Taylor series expansion keeping only the first order term:

$$(x'-X)=\lambda(x-X) \qquad [2.22]$$

where $\lambda=df(x)/dx$ evaluated at x=X is an eigenvalue associated with the fixed point. If we set X=-1

$$\lambda 1=[df(x)/dx]\Big|_{x=-1}=2$$

Setting X=0,1/2, we get

$$\lambda 2=[df(x)/dx]\Big|=0$$

$$\lambda 2=[df(x)/dx]\Big|_{x=0} \quad =0$$

$$\lambda 3=[df(x)/dx]\Big|_{x=1/2} \quad =4$$

Given the three eigenvalues ($\lambda 1,\lambda 2,\lambda 3$) we can predict whether the fixed points X are stable or unstable. In general, when $|\lambda|<1$, the eigenvalue is said to be "irrelevant" and the fixed point is stable, for $|\lambda|=1$, the eigenvalue is said to be "marginal", and for $|\lambda|>1$ the eigenvalue is said to be "relevant" and the fixed point is unstable. A stable point corresponds to a λ value where x from equation [2.22] does not move away from X (i.e. $x-X=0$). In our case, a stable point occurs when $\lambda 2=0$; we see that $(x-X)=0$ at all stages of iteration. An unstable point occurs when $\lambda 3=4$, x moves farther and farther away from X after each stage of iteration. It is the latter type of eigenvalue that we are generally interested in as will be seen below.

The fixed points describe the singularities of the Green's function G. That is, near the fixed points ($X=V/Ec$) there exists a critical energy Ec where

$$G(i) \propto [E-Ec]^{(d-y)/y} \qquad [2.23]$$

Figure 2.2:
The Green's function $[(-1/\pi)G(0)]$ for the vibrational problem (ϵ=2V) of the uniform chain with the real and imaginary part (stars and squares respectively) plotted as a function of energy E. The density of states is given by the imaginary part of the Green's function.

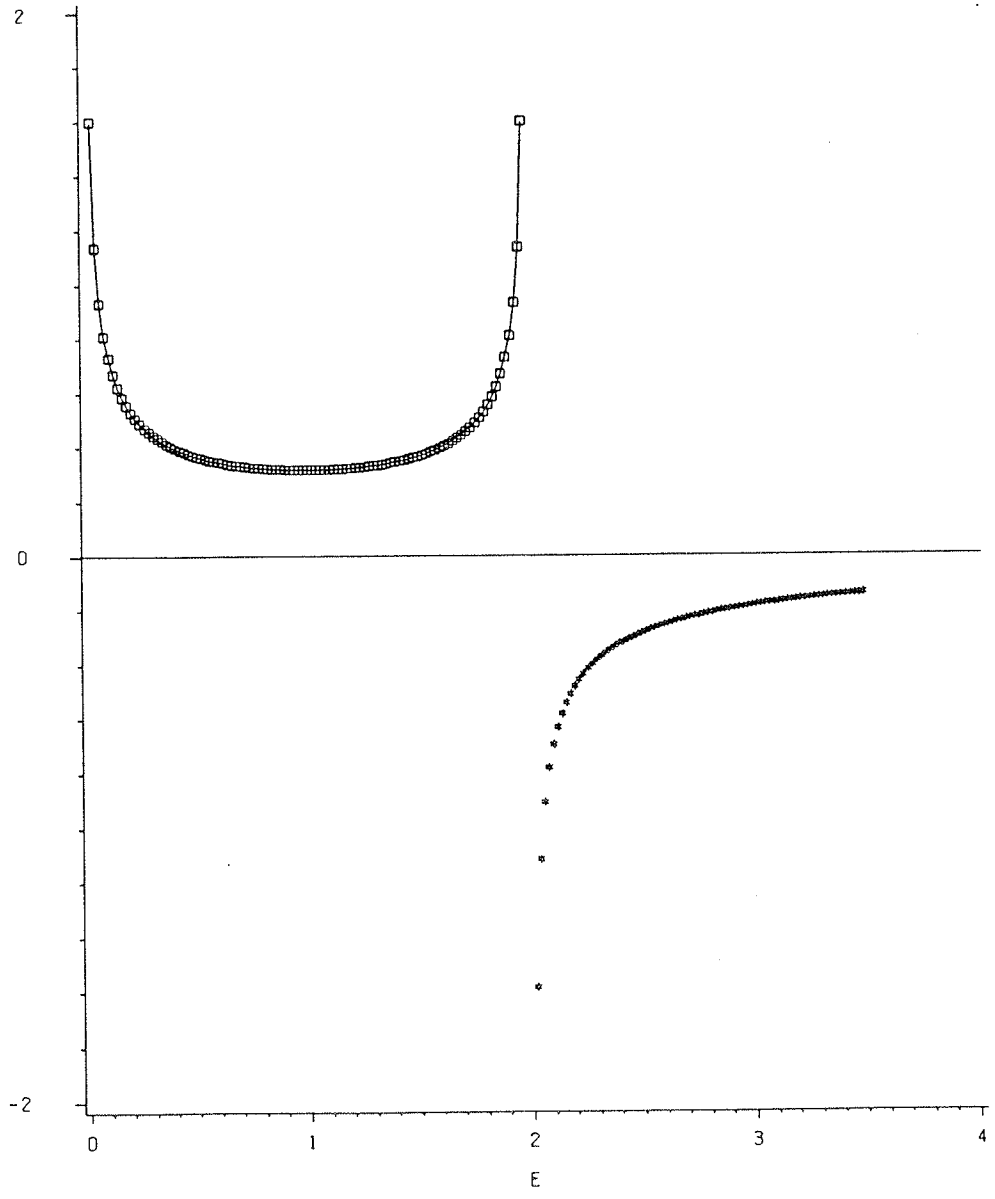

The parameter "d" is the Euclidean dimension of the system and "y" is an exponent corresponding to the largest eigenvalue of the associated fixed point. For a scaling factor that we denote as b, the eigenvalues are of the form

$$\lambda = b^{y} \qquad [2.24]$$

In the one-dimensional chain, we scaled our system by a factor of two (b=2) so that for our critical point X=1/2, which had the largest eigenvalue $\lambda=4$, the exponent will be y=2. The point X=1/2 will give a corresponding critical energy $Ec=\epsilon+2V$ and the Green's function for E values close to Ec will behave as follows

$$G(i) \propto [E-Ec]^{-1/2} \qquad [2.25]$$

which tells us that the divergence of G(i) at E=Ec is an inverse square root and represents a band edge as shown in figure 2.2. In fact, this value of $Ec=\epsilon+2V$ corresponds to the upper band edge of the linear chain. The lower band edge $Ec=\epsilon-2V$ corresponds to X=-1/2 which maps onto X=1/2 in one iteration and hence has the same type of singularity.

The scaling approach described above can also be used for systems without translational invariance. For instance, if

we introduce a single impurity in the linear chain, the translational invariance will be destroyed by the disorder and the average density of states of the system is no longer equal to the density of states at each site. The solution for G(i,i) at the impurity site is now different from the other G's since $G(i,j) \neq G(|i-j|)$ and equation [2.18] is no longer valid. We must evaluate each G(i,i) separately. The impurity site itself has a different energy parameter $\epsilon(i)$ including a different coupling constant V(i,k) (assuming that the impurity interacts only with its nearest neighbour) while the remainder of the sites have the same energy ϵ and the same coupling constant V as before. A set of renormalized parameters can be obtained for the impure system as was done for the pure case. Included in this set though is the "x" parameter from equation [2.13] because beyond a certain range of the impurity (three neighbouring atoms),the remainder of the lattice behaves like a uniform chain. If we let i=0 denote the site of the impurity, the local density of states will be different from the other sites in that a local or isolated mode exists beyond the continuous band as shown in figure 2.3. Increasing the number of impurity sites makes the calculation of the average Green's function much more difficult. We must consider interactions that can exist between impurities themselves and we must also consider the interactions between the impurities with the remainder of the sites. The number of local modes will also increase if we increase the

Figure 2.3: The Green's function $[(-1/\pi)G(0,0)]$ with a single mass defect where the impurity is lighter than the host atoms. The real and imaginary parts (stars and squares respectively) are plotted as a function of energy E. Note that this defect produces a localized mode outside the band edge if we compare with figure 2.2.

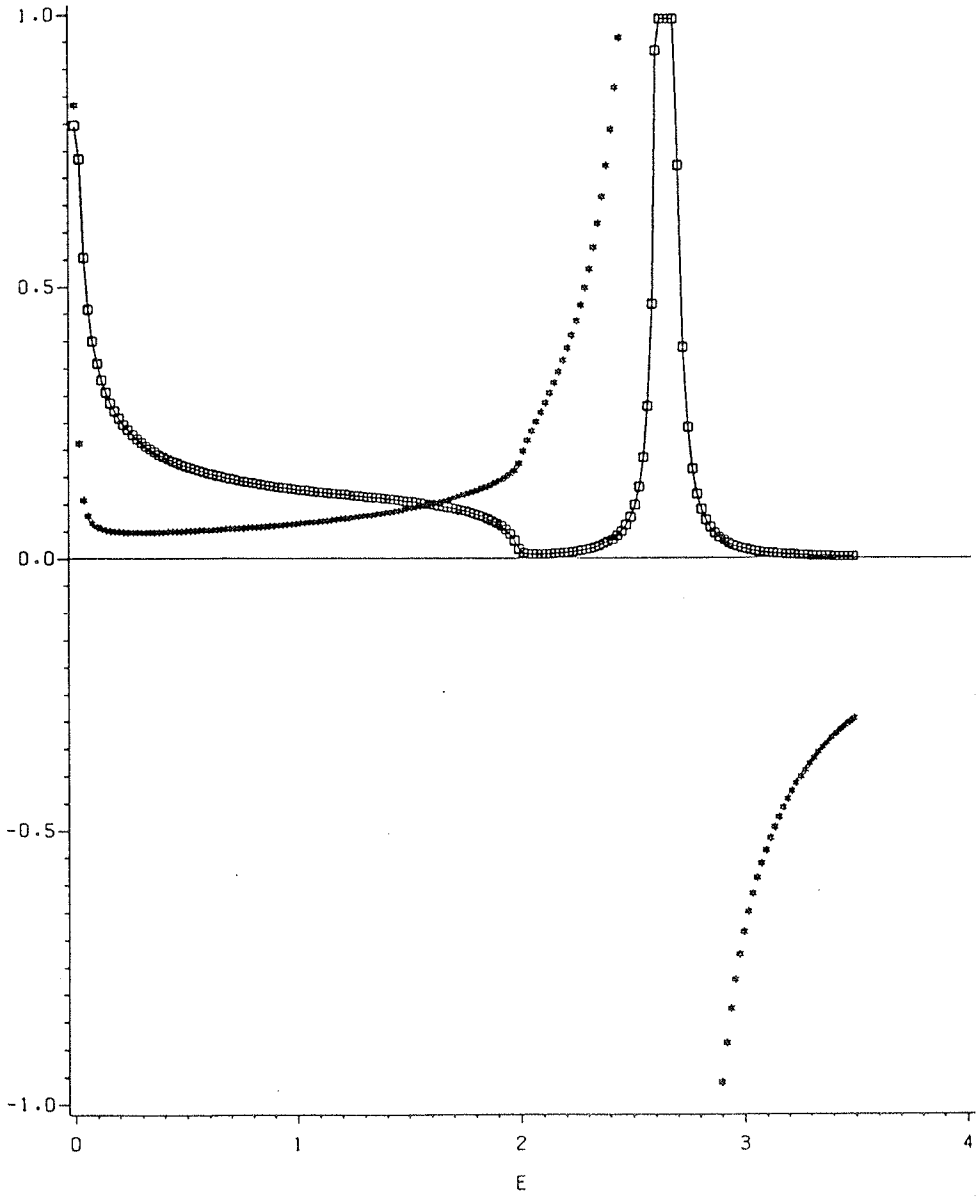

concentration of these impurities and in one dimension, all excitations produced by the impurities are localized.

However the fact that all the excitations in one dimension are localized does not mean that all excitations will be localized for two- or three-dimensional systems. In these cases, it is believed that only if the "strength" of the disorder exceeds a certain value do all the eigenfunctions become localized (Anderson, 1958). This means that we cannot expect to find extended states analogous to the Bloch functions of an ordered crystal. The point at which this transition occurs,which is known as the "Anderson Transition", is difficult to determine for any system although there is no doubt that such a transition does exist. This behaviour of the Anderson model has been deduced from both theoretical and numerical studies. The model is expressed in terms of a TBH where each ϵ is taken to be an independent random variable.

The Anderson model is quite general in that it is applicable to disordered systems where the disorder is uniformly distributed throughout the system. We shall consider a more specific case, namely the binary alloy, where we have two types of atoms:some with infinite mass ("heavy" atoms) and some with light mass ("light" atoms). For simplicity, we assume that we have a lattice with all sites originally occupied by heavy atoms (note that there are no vibrational modes for such atoms because of their

infinite mass). Our light atoms will be considered the impurity atoms as we randomly substitute light atoms for heavy ones. It is evident that when the concentration of these impurities is small, the probability of their localized states overlapping will also be small. Obviously, increasing the concentration will increase the chances of these states overlapping. In fact, depending on how these impurities occupy sites on the lattice, which is purely a geometrical problem, this will tell us whether or not localized states will overlap. For instance, suppose that we have a single impurity in a lattice and then introduce another impurity atom close to it (as nearest neighbours) so that their localized states overlap. Increasing the number of impurities makes it more probable that these localized states will combine to produce a more "delocalized" state. If the impurity concentration increases to a point, where we have an uninterrupted path of nearest neighbour impurity atoms from one end of the lattice to the other, then the localized states of these atoms will overlap and combine to form extended state(s). These atoms that form this path are said to be a member of an "infinite cluster". There exists of course isolated groups of atoms that are not part of this infinite cluster and which exhibit localized properties. However, these isolated groups become part of the infinite cluster as the concentration of impurity atoms is further increased.

The connection that we would like to make between the problem above and the Anderson model is contained in the following question: will extended states be formed at any concentration of the impurities (with some finite probability) or does there exist some critical value of impurity concentration analogous to the Anderson transition as we go from localized states to extended states? This binary mass problem is equivalent to the classical percolation problem (Broadbent and Hammersley, 1951), where atoms are distributed randomly on sites with a probability "p". The question that is addressed in percolation is: what is the probability P(p) of an atom belonging to an infinite cluster? In a one dimensional chain it is clear that an infinite cluster is formed only if p=1. However this is not true in higher dimensions.

2.2 PERCOLATION

The percolation model is a purely geometrical problem which can be described in the following way (Stauffer, 1979; Essam, 1980): imagine we have a lattice in which each lattice site can either be occupied or unoccupied by an atom. Assume that the occupation of a site by an atom is entirely a random process and is not influenced by the presence of other occupied sites around it. We then introduce a parameter "p", where p is the probability of an atom occupying a certain site on the lattice and (1-p) is

the probability of the site not being occupied,the probability of occupation being the same for all lattice sites. We can also consider the probability of sites being connected by bonds. Thus p can stand to mean the probability of a bond existing between neighbouring sites or (1-p) that the bond is not there. Hence depending on the problem at hand, it might be convenient to choose a bond percolation approach rather than site percolation. It is this parameter p which represents the fraction of occupied sites or bonds in the lattice.

In the percolation problem, the occupied sites are either isolated from each other or they can form small groups of neighbouring sites called "clusters". We define a cluster to be a group of occupied lattice sites connected by nearest neighbour distances and we let "s" represent the number of sites in the cluster. Figure 2.4 gives an example of the application of the percolation model to a square lattice. The general features of the cluster as a function of p are thus apparent: if p is close to zero, the occupied sites will be isolated from each other and if p is close to unity,then clearly we see that nearly all occupied sites are connected to each other and form one large cluster extending from one end of the lattice to the other. For systems that are "infinite" in extent, the large cluster is said to be an "infinite" cluster. Hence a clear distinction exists for large lattices: either an "infinite" cluster exists,or it doesn't. Notice that an infinite cluster appears when p=0.6.

Figure 2.4: Examples for percolation on a 20X20 square lattice, for p=0.1,0.2,...0.9. Occupied sites are shown as crosses,empty sites are not shown. The ovelapping crosses at 60 percent probability give the largest "percolating" cluster (Stauffer,1979).

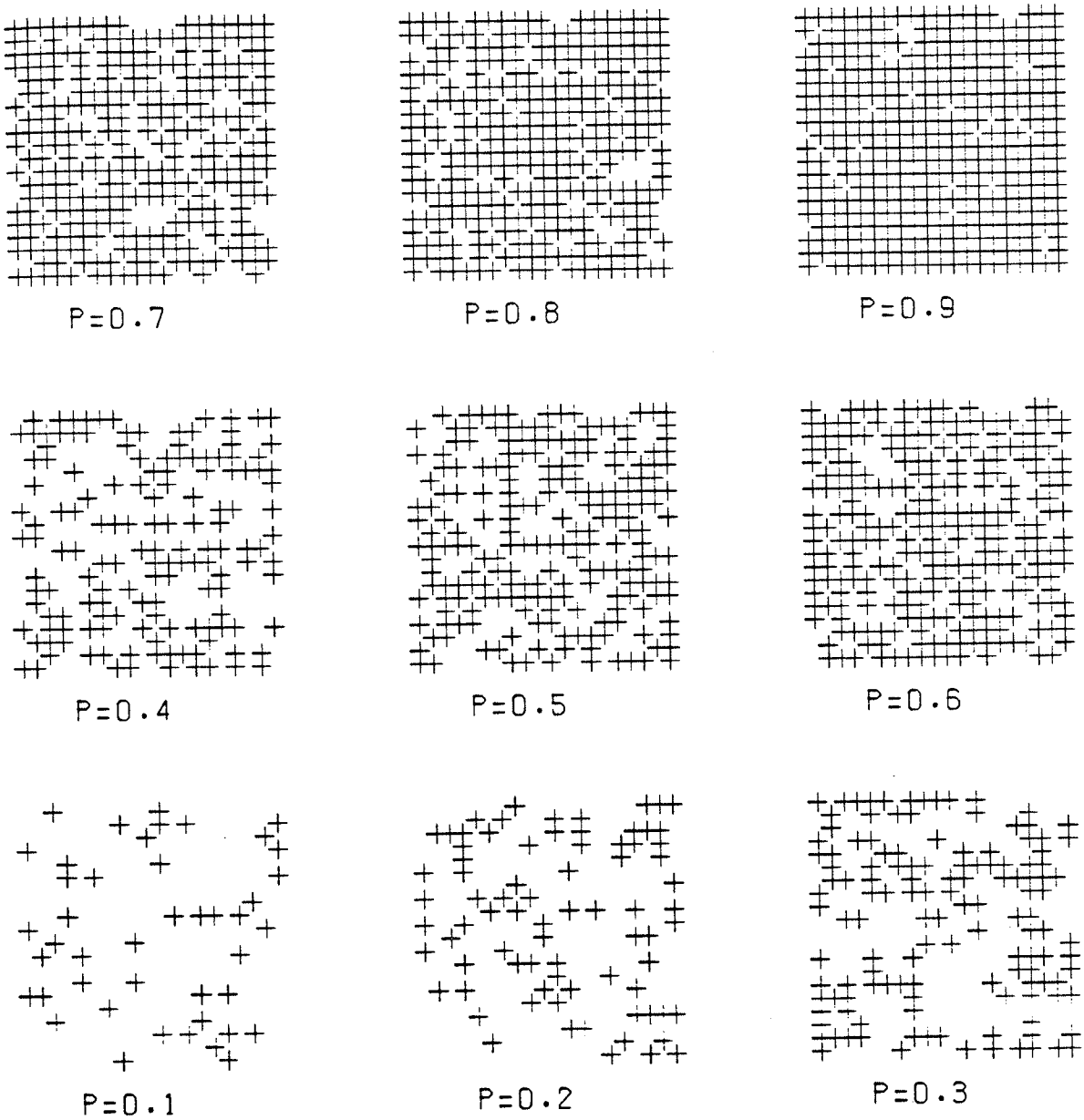

We introduce a parameter "Pc" which is defined as the percolation threshold and is the critical value of p where for the first time an infinite network percolates through a lattice with finite probability. One could say that a phase transition occurs at Pc: for p above Pc a percolating network exists and for p below Pc no percolating network exists. One might expect that an infinite cluster could be formed for very low p's, a square lattice for instance can have a straight line of connected sites extending from one end of the lattice to the other. However, one should keep in mind that such an arrangement has an extremely low probability of occuring in a random distribution of occupied sites on a large lattice. A physical example to consider is an electrical network of resistors (Thouless, 1978; Zallen, 1983). We take a square netting of resistors and apply a potential difference across both ends. Then by snipping resistor leads at random which corresponds to removing bonds in a lattice with probability p, a point will be reached where no current whatsoever will pass through the grid. This point would denote a critical or threshold point which would correspond to Pc.

The percolation model is thus concerned with the behaviour of the percolation probability "P(p)" as a function of p. It is one of several quantities that is used in the percolation model. It denotes the probability of occupied sites belonging to the infinite percolating

cluster. The distinguishing property of P(p) is that it vanishes to zero at Pc and is non-zero above Pc (see figure 2.5). This behaviour of P(p) is similar to the behaviour of the magnetization near a magnetic phase transition. The manner in which P(p) vanishes near Pc defines a critical exponent β as follows

$$(p-Pc)\rightarrow 0 \; : \; P(p) \propto (p-Pc)^{\beta} \qquad [2.26]$$

Another quantity that is of interest to us is the correlation length "ξ" of the cluster. It is defined as the maximum separation of two sites (or bonds) in the cluster

$$\xi=\max\{|r(i)-r(j)|\} \; i,j \text{ in the cluster} \qquad [2.27]$$

By averaging ξ over <u>all</u> <u>finite</u> clusters we obtain the mean cluster spanning length $<\xi(p)>$ which is a function of p; its analogue is the correlation length in phase transitions. It's behaviour near Pc also defines a critical exponent (υ)

$$<\xi(p)> \propto |p-Pc|^{-\upsilon} \qquad [2.28]$$

Figure 2.5: The percolation probability P(p) (solid line) is zero at Pc and is equal to 1.0 when p=1.0. The average correlation length $\langle \xi(p) \rangle$ (dash line) is finite (or zero) at p=0.0 and at 1.0 but diverges when p=Pc.

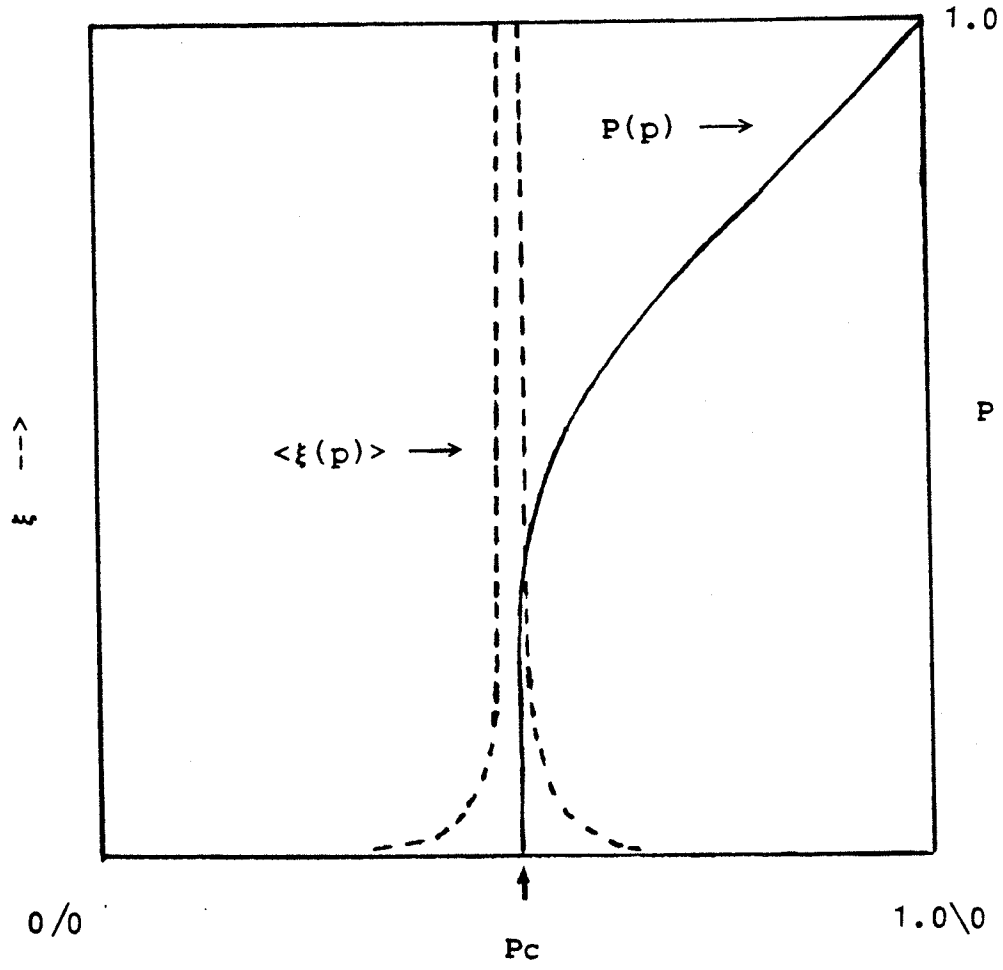

$\langle\xi(p)\rangle$ is finite above and below Pc and diverges at Pc (see figure 2.5) whereas P(p) is zero at and below Pc and finite above Pc. Thus $\langle\xi(p)\rangle$ describes the geometric aspects of growth of clusters below Pc. It is known from numerical calculations (Gefen et al, 1981) that for length scales well above ξ the infinite cluster appears homogeneous and that for length scales below ξ but well above the lattice spacing the cluster appears self-similar (i.e. the cluster will appear the same when viewed at different magnifications providing that we cannot distinguish the lattice spacings).

We normally think of a d-dimensional Euclidean object being bounded by a (d-1)-dimensional surface and we normally expect the surface/volume ratio to go to zero as the size of the object goes to infinity. This does not happen for a percolation cluster. The ratio of the size of the boundary surrounding the cluster to the volume of the cluster itself is found to approach a limiting value as the number of sites in the cluster increases. It has been shown by experiment that for large clusters, the average relationship between the cluster mass "s" and the correlation length ξ is described by the following power law

$$s(\#\text{ of occupied sites}) \propto \xi^{D} \qquad [2.29]$$

Normally one would expect D to be the Euclidean dimension d but numerical results have determined D to be non-integral and hence the cluster is said to have a fractional dimension. The above equation relates a length dimension, ξ, with a measure of content or mass,s. It gives us a way of characterizing the "stringy" or "lacy" structures that are inherent in percolation clusters. To determine the value of D, we can calculate the mass of the infinite cluster by using the density (=mass/volume). Consider a region of space whose dimensions are of the order of the correlation length ξ and which encloses a volume ξ^d. The probability of a site belonging to an infinite cluster is P(p) and using equations [2.26] and [2.28], the total number of sites in this region is

$$\text{mass=density x volume}$$

$$\xi^D \propto P(p) x \xi^d$$

$$\xi^D \propto \xi^{d-\beta/\upsilon}$$

This allows us to make the following connection between the cluster dimension D and the Euclidean dimension

$$D=d-\beta/\upsilon \qquad [2.30]$$

The peculiar nature of the structure of clusters has lead to the study and application of these geometric shapes to model disordered lattices. These apparently "non-Euclidean" objects are named "fractals", a term coined by Mandelbrot (1977) and we will be using "fractals" to model disordered systems. In particular, we will employ a certain class of fractals known as self-similar fractals.

2.3 FRACTALS

Fractals are geometric shapes of fractional dimensionality (Mandelbrot, 1979). They are not translationally invariant but they can be scale invariant, that is, each piece of a straight segment is like a reduced scale version of the whole. Scale invariant also means that by looking at a fractal at increasingly higher resolution, increasing amounts of detail are revealed that are scaled versions of the variations seen at lower resolution; they "appear" to have order even though they are not translationally invariant. These types of fractals that give an appearance of order are known as "self-similar" fractals. Many self-similar fractals can be constructed by recursive replacement of segments,triangles,squares etc. by more complex shapes called "generators" which are themselves segments,triangles,squares etc. This method of constructing fractals is what gives them their non-integer dimensionality.

Figure 2.6:
a) The two dimensional Sierpinski Gasket.
b) The three dimensional Sierpinski Gasket.

(a)

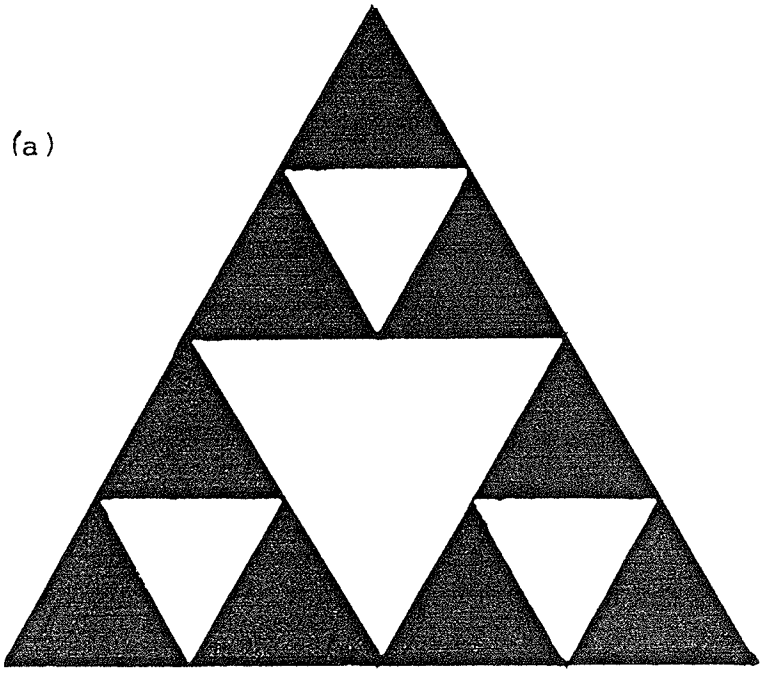

(b)

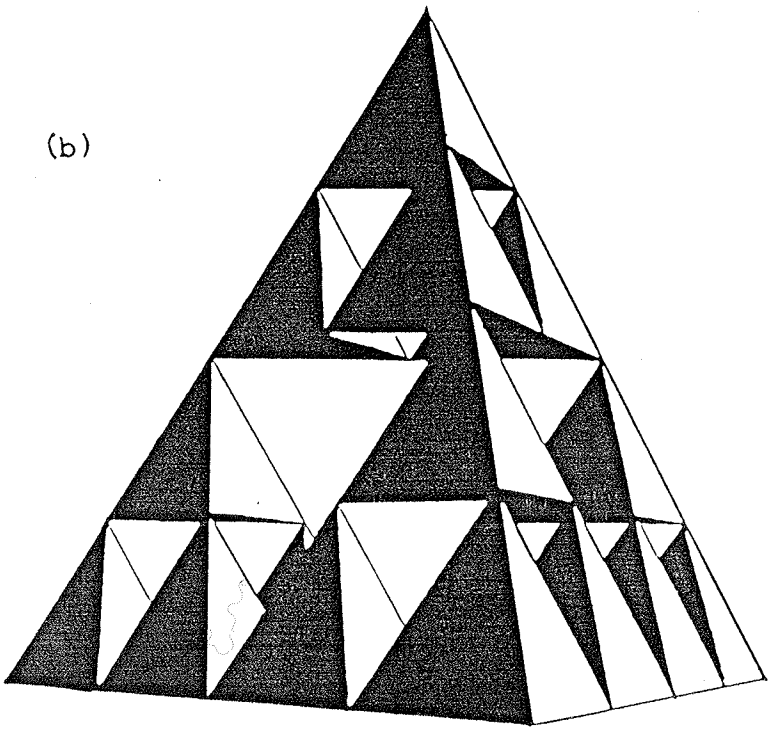

The two fractal objects that are of interest to us are the two and three dimensional Sierpinski gaskets given in figure 2.6. In the two dimensional case, we begin with a triangle, and use a triangle as a generator. We divide each triangle into four smaller equilateral triangles and remove the central triangle. We can keep doing this recursively for the remaining triangles until we get the desired fractal shape. Notice in figure 2.6 that certain regions on a small length scale look identical to other regions of larger length when magnified. This is what's known as the self-similarity of the fractal. Similarly for the three-dimensional case, we start off with a tetrahedron and use a tetrahedron as a generator. We divide the tetrahedron into eight smaller tetrahedrons and remove the central four as shown in figure 2.6. The fractal dimensionality D of these objects are obtained from the general expression (Mandelbrot, 1979)

$$D=\ln(N)/\ln(b) \qquad [2.31]$$

where we recursively replace each segment by "N" smaller segments of length 1/b. For the Sierpinski gaskets, D is of the form (Gefen et al, 1981)

$$D=\ln(1+d)/\ln(2) \qquad [2.32]$$

where d is the Euclidean dimension. If d=2 (the 2-d gasket), then D=1.585 and if d=3 (the 3-d gasket), then D=2.0. Note that for all fractal lattices D is always less than its corresponding Euclidean dimension d.

Fractals have been useful in the interpretation of the behaviour of certain real systems such as polymers, epoxy resins and glasses (Derrida et al, 1984). They are particularly useful for modeling disorder in pure systems since they are not translationally invariant. The physical properties of such systems can be obtained by calculating the density of states. In the next chapter, we will use the 2-d and 3-d Sierpinski fractals as a way of modeling disorder in certain lattices. We will see how disorder in a pure system destroys the smoothness of the spectra of these pure systems. However, in order to calculate such spectra we will employ a generating function technique.

2.4 GENERATING FUNCTION

As mentioned in section 1.1, the calculation of the average density of states in disordered systems involves calculating all the G(i,i)'s. However, this problem can be avoided by using a complex generating function (Tremblay and Southern, 1983) which exploits the renormalization group method. We begin by expressing the eigenstates $|\psi\rangle$ of the TBH in the following form

$$|\psi\rangle=\sum_i u(i)|i\rangle \qquad [2.33]$$

where the u(i)'s are continuous variables and represent amplitudes on each site of the lattice. The TBH acts on the elements u(i) as follows

$$Hu(i)=\epsilon u(i) + V[u(i+1)+u(i-1)] \qquad [2.34]$$

where again we assume nearest neighbour interactions. Consider the following functional integral,

$$F=\ln\{\int Du\ \exp(iS)\} \qquad [2.35a]$$

where

$$S= (1/2)U^+(E-H)U= (1/2)(E-\epsilon)\sum_i u(i)^2 - \sum_{i\neq j} V(i,j)u(i)u(j) \qquad [2.35b]$$

with

$$\int Du=\prod_{i=1}^{N}\int du(i) \qquad [2.36]$$

and

$$U^+=\{u(1),u(2),\ldots,u(N)\} \qquad [2.37]$$

where z=E+is and s is a positive number that ensures convergence of the integral. It is easily shown that F is a generating function for the Green's function equations [1.9] (see appendix A) where

$$G(l,m)=-i\{\int Du\ u(l)u(m)\exp(iS)\}[\int Du\ \exp(iS)]^{-1} \qquad [2.38]$$

If we differentiate F w.r.t. E, then we obtain

$$\partial F/\partial E=-(1/2)\sum_i G(i,i) \qquad [2.39]$$

The off-diagonal term G(i,j) can also be obtained from F as follows

$$G(i,j)=\partial F/\partial v(i,j) \qquad [2.40]$$

The average density of states from equation [1.6] becomes

$$\rho(E)=(1/N)(2/\pi)\lim_{s\to 0}\{Im[dF(z)/dE]\} \qquad [2.41]$$

and the cumulated or integrated density of states in equation [1.8] can be expressed as follows

$$N(E)=\int\rho(E)dE=(1/N)(2/\pi)\lim_{s\to 0}\{Im[F(z)]\} \qquad [2.42]$$

In the next section, we will use equations [2.41] and [2.42] to evaluate the average density of states for systems without translational invariance. This technique avoids the problem of calculating all the G(i,i) separately and allows us to calculate $\rho(E)$ directly from F.

3 FRACTAL LATTICES AS MODELS OF DISORDER

In this chapter, we will describe a model of a disordered system and calculate the spectral properties using a functional integral approach. We shall study the triangular lattice in two dimensions and the face-centered cubic (FCC) lattice in three dimensions. The disordered state of each lattice will be achieved by embedding a fractal structure in them on small length scales. The structures will have a self-similar geometry on scales of length from the nearest neighbour distance "a" up to some larger length scale "L". Beyond this latter length scale, the lattice has a regular homogeneous structure. In this way, we hope to model the essential geometrical features of disordered lattices which have been found in the studies of percolation clusters. We will determine both the density of states and the integrated density of states of a TBH on these disordered systems by using the generating function described in section 2.5. The triangular lattice is treated in somewhat more detail than the FCC since most of the results we derive in two dimensions are directly applicable to three dimensions.

3.1 2-D TRIANGULAR LATTICE

In figure 3.1a, we consider a portion of a regular triangular lattice and denote the lattice spacings on this scale by "L". The lattice consists of both upward and downward pointing triangles. Within each "up" triangle, we generate additional sites and bonds as for the Sierpinski fractal in section 2.3. Figures 3.1b,c show the first (n=1) and second (n=2) iterations of this procedure. At each stage, the new nearest neighbour distance "a" is related to L by

$$L=2^{n}a \qquad [3.1]$$

where n is the number of times we have iterated. Note that holes exist in our disordered system which are the size (L) of those triangles with no fractal structure. Percolation clusters above Pc have a similar geometry with the correlation length ξ representing the distance between nodes in the infinite cluster. We identify this length with the distance L between the sites of our pure triangular lattice. Hence in our model

$$\xi=2^{n}a \qquad [3.2]$$

Figure 3.1:
a) A section of a pure triangular lattice for n=0.
b) The same section with disorder for n=1.
c) The same section with disorder for n=2.

(a)

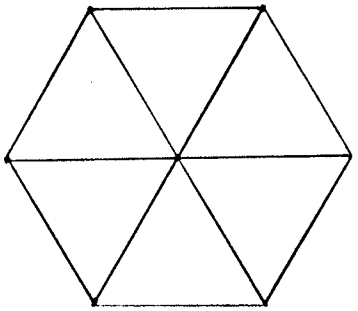

(b)

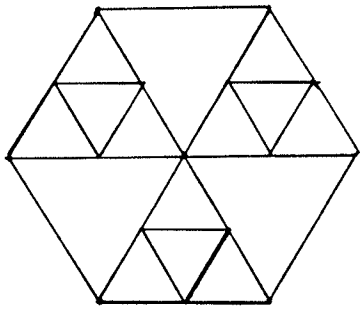

(c)

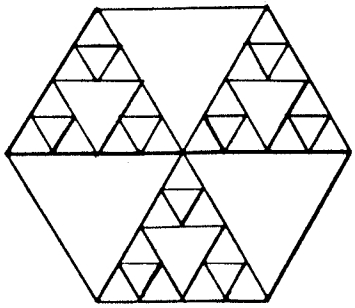

We point out that our disordered lattice does not have any "dangling" bonds or bonds with dead ends as in figure 2.4. Hence our model only describes what is called the "backbone" of the percolation cluster. As shown in figure 3.1, we consider the disorder to be self-similar for length scales above the lattice spacing "a" and below the correlation length ξ. On the other hand, for lengths above ξ, the system is homogeneous and is translationally invariant. As n increases, the reduced correlation length ξ/a diverges and the structure is self-similar on all scales. Hence $n=\infty$ corresponds to the system approaching the percolation concentration Pc whereas n=0 corresponds to p=1. By changing n, we can investigate the spectral properties of the system as a function of p-Pc.

We can relate p-Pc to n as follows: consider a pure lattice with N sites . Since there are N upward pointing triangles, we associate one Sierpinski gasket with each lattice site. At each stage of iteration the number of triangles can be increased by a factor of (2^d) but we only keep (d+1) of them so that the ratio of these two quantities gives the probability of a site belonging to the infinite cluster. For the triangular lattice, d=2 but the same result can be used for the FCC lattice with d=3. The percolation probability is thus

$$P(p)=[(d+1)/2^d]^n \qquad [3.3]$$

If we assume that P(p) has the scaling form given by equation [2.26] for all Pc<p<1, then

$$P(p)=[(p-Pc)/(1-Pc)]^{\beta} \qquad [3.4]$$

Using the fractal dimension as defined in equation [2.32] and equating equations [3.3] and [3.4] above, we find

$$p=Pc + (1-Pc)(2^{D-d})^{n/\beta} \qquad [3.5]$$

If we also assume that the correlation length has the same scaling form given by equation [2.28] for all Pc<p<1, then

$$\xi(p)=a[(p-Pc)/(1-Pc)]^{-\upsilon}=2^{n}a \qquad [3.6]$$

yielding

$$p=Pc + (1-Pc)2^{-n/\upsilon} \qquad [3.7]$$

Equations [3.5] and [3.7] are consistent only if $D=d-\beta/\upsilon$. This can be taken as the definition of the dimension of our clusters provided we use values of β and υ appropriate for the backbone (Gefen et al, 1981). The value of Pc in two

dimensions is that for the bond percolation problem on the triangular lattice and has the value Pc=0.3473 whereas for the FCC lattice the value of Pc is 0.199 (see Stauffer, 1979).

To calculate the spectral properties of our disordered system, we use the TBH and use the same conditions given in equations [2.1a,b]. Although these are the same conditions that one would impose on a uniform system where the atoms are all the same, our system is disordered due to the lack of translational invariance so that we cannot use the Fourier transform approach for this problem.

To calculate the average Green's function, we must use the functional integral approach described in section 2.5. Employing the ideas of the renormalization group technique described in section 2.1, we begin by considering the row vector in equation [2.37] and we partition the u(i)'s into two groups: one group, U_1, contains the sites we want to keep at each stage and the other group, U_2, contains the sites that we want to eliminate. In this basis, the term $U^*[zI-H]U$ in F can be rewritten as

$$[U_1,\ U_2] \begin{bmatrix} z-H_{11} & -H_{12} \\ -H_{21} & z-H_{22} \end{bmatrix} \begin{bmatrix} U_1 \\ U_2 \end{bmatrix} \qquad [3.8]$$

where $z=E+is$. We now define new vectors $\tilde{U}_1$ and $\tilde{U}_2$ as follows

$$\tilde{U}_1 = U_1 \qquad [3.9a]$$

$$\tilde{U}_2 = U_2 - (zI - H_{22})^{-1} H_{21} U_1 \qquad [3.9b]$$

After some algebraic manipulation we have

$$(i/2)U^+(zI-H)U = (i/2)\{\tilde{U}_1^+(zI-H_{11}')\tilde{U}_1 + \tilde{U}_2^+(zI-H_{22})\tilde{U}_2\} \qquad [3.10]$$

where

$$H_{11}' = H_{11} + H_{12}(zI-H_{22})^{-1}H_{21} \qquad [3.11]$$

The Jacobian of the transformation [3.9] is unity and we can perform the integration over the U_2 variables to obtain

$$F = \int Du \exp\{(i/2)\tilde{U}_1^+[zI-H_{11}']\tilde{U}_1\} + Q \qquad [3.12]$$

where the constant of integration Q is

$$Q = (-1/2)\ln\{\det[zI-H_{22}] + [(N-N')/2]\ln(2\pi i)\} \qquad [3.13]$$

In the first term of equation [3.12], the integral must still be performed over the N' uneliminated sites and N denotes the total number of sites in the lattice (N>N') before each elimination. This term represents the generating function for a new system with fewer degrees of freedom and with new effective interactions described by equation [3.11]. This elimination process can be repeated simply by iterating equations [3.11]-[3.13]. Hence F can be expressed after k iterations (or integrations) in the following form

$$F=F_K+Q(1)+Q(2)+...+Q(k-1) \qquad [3.14]$$

where after each stage "k" of iteration we have

$$H_{11}(k)=H_{11}(k-1) + H_{12}(k-1)[zI-H_{22}(k-1)]^{-1}H_{21}(k-1) \qquad [3.15]$$

and

$$Q(k)=(-1/2)\ln\{\det[zI-H_{22}(k)]\} + (1/2)[N(k)-N(k+1)]\ln(2\pi i) \qquad [3.16]$$

where N(k) is the number of sites left after k iterations. The last term in equation [3.16] is a constant which we shall neglect from now on. The term F_K in equation [3.14] represents the generating function of the remaining sites in

the lattice. We can evaluate the average Green's function at the k'th iteration as follows

$$\langle G(0)\rangle = [-2/N(0)]dF/dE$$
$$= [-2/N(0)]\{dF_K/dE + \Sigma dQ(m)/dE\} \qquad [3.17]$$

where N(0) is the total number of sites on the lattice initially.

We now consider a section of a fractal lattice that has been constructed as in figure 3.1 after "n" iterations with a total of N(0) sites. We divide these sites into two unequal groups as follows: the group belonging to U_2 are the sites on the smallest scale and the remaining sites belonging to U_1 are those that have been generated by only (n-1) iterations. As is easily seen from figure 3.1, the sites which are being eliminated at each stage form $(N-N')/N_b$ independent blocks of $N_b=3$. Hence the evaluation of equations [3.11] and [3.13] simplify. Figure 3.2 shows one of these blocks and the three remaining sites with which they interact. The matrix elements of (zI-H) in this basis can be written as follows

$$zI-H = \begin{bmatrix} z-\epsilon & 0 & 0 & -V & -V & 0 \\ 0 & z-\epsilon & 0 & 0 & -V & -V \\ 0 & 0 & z-\epsilon & -V & 0 & -V \\ -V & 0 & -V & z-\epsilon & -V & -V \\ -V & -V & 0 & -V & z-\epsilon & -V \\ 0 & -V & -V & -V & -V & z-\epsilon \end{bmatrix} \qquad [3.18]$$

Figure 3.2:
a) This is a block (N_b=3) of sites used to obtain the matrix elements of zI-H.
b) The same block after sites have been eliminated.

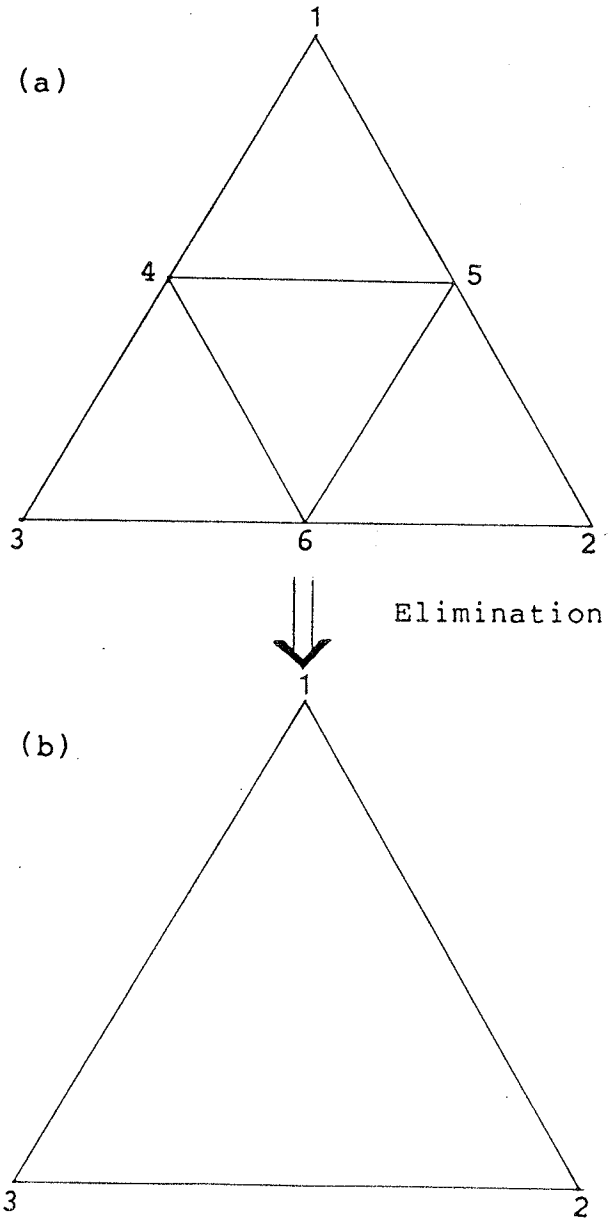

The sites (1,2,3) in figure 3.2 will also interact with another block of three not shown in the diagram. However, each bloch contributes equally to the renormalized energy of these sites and we multiply the renormalized energy parameter by a factor (q=2). The renormalized parameters are thus obtained by partitioning the matrix H in the following way

$$H_{11}=\begin{bmatrix}\epsilon & 0 & 0\\ 0 & \epsilon & 0\\ 0 & 0 & \epsilon\end{bmatrix} \quad H_{12}=\begin{bmatrix}V & V & 0\\ 0 & V & V\\ V & 0 & V\end{bmatrix}$$

[3.19]

$$H_{21}=\begin{bmatrix}V & 0 & V\\ V & V & 0\\ 0 & V & V\end{bmatrix} \quad H_{22}=\begin{bmatrix}\epsilon & V & V\\ V & \epsilon & V\\ V & V & \epsilon\end{bmatrix}$$

Using equation [3.11], we find the following renormalized parameters

$$H_{11}'=\begin{bmatrix}\epsilon' & V' & V'\\ V' & \epsilon' & V'\\ V' & V' & \epsilon'\end{bmatrix} \qquad [3.20]$$

where

$$\epsilon' = \epsilon + \{q2V^2(z-\epsilon+V)(z-\epsilon)\}/[(z-\epsilon)^3-3(z-\epsilon)V^2-2V^3] \quad [3.21a]$$

$$V' = V^2\{(z-\epsilon+2V)(V+z-\epsilon)\}/[(z-\epsilon)^3-3(z-\epsilon)V^2-2V^3] \quad [3.21b]$$

Setting $x=V/(z-\epsilon)$, we get ϵ', V', and x' in terms of x:

$$(z-\epsilon') = (z-\epsilon)\{1-(4x^2)/[(1+x)(1-2x)]\} \quad [3.22a]$$

$$V' = V\{[x(1+2x)]/[(1+x)(1-2x)]\} \quad [3.22b]$$

$$x' = x^2/(1-3x) \quad [3.22c]$$

We can also write equation [3.13] as

$$Q = -[(N-N')/2N_b]\ln\{\det[zI-H_{22}]\} \quad [3.23a]$$

where

$$\det(zI-H_{22}) = (z-\epsilon)^3[(1+x)^2(1-2x)] \quad [3.23b]$$

is the determinant of <u>each block</u>. When we consider the whole lattice, we must include another renormalized

parameter, denoted as "ϵ_c", which is the corner site energy. The corner sites are the sites that belong to the pure triangular lattice and it is easily seen from figure 3.1 that these sites interact with three other blocks (q_c =3). Elimination of these blocks yields a renormalized parameter value for ϵ

$$\epsilon_c' = \epsilon_c - (q_c 2Vx)/[1-x-2x^2] \qquad [3.24]$$

The dimensionless quantity $x_c = V/(z-\epsilon_c)$ can be expressed as

$$x_c' = [(x_c)x(1+2x)]/[(1+x)(1-2x)-6x(x_c)] \qquad [3.25]$$

Once we have eliminated all sites on scales from "a" to ξ, we are left with a uniform triangular lattice with tight binding parameters ϵ_c and V obtained by iterating equations [3.22] and [3.24] "n" times. However, both ϵ_c and V at this stage are non-linear functions of the <u>initial</u> energy E. We are now in the position to determine the form of dF(n)/dE in equation [3.17] where F(n) is the contribution from the pure lattice to the total F. Using the chain rule of differentiation, we have for the total derivative of F(n)

$$dF(n)/dE = [\partial F(n)/\partial Ec(n)][dEc(n)/dE] + [\partial F(n)/\partial V(n)][dV(n)/dE] \qquad [3.26]$$

where $Ec(n)=E-\epsilon(n)$. Since the remaining sites form a homogeneous lattice, we can use equations [2.39] and [2.40] to express $dF(n)/dEc(n)$ and $dF(n)/dV(n)$ in terms of G0 and G1 where G0 and G1 are the diagonal and nearest neighbour Green's function of the pure lattice. We then use $(E-\epsilon)G0=1+zV(n)G1$ to finally obtain

$$dF(n)/dE=-[N(n)/2]\{(G0)V(n)d[Ec(n)/V(n)]/dE + d[\ln V(n)]/dE\} \quad [3.27]$$

The diagonal Green's function G0 for the triangular lattice has been calculated by Horiguchi (1972). The derivatives in equation [3.17] and [3.26] are easily evaluated using equations [3.22]-[3.24]. If the initial disordered system has been constructed using "n" iterations of the Sierpinski gasket on a triangular lattice with N sites, then the total number of sites at any stage k is

$$N(k)=N[(3^{n-k+1}-1)/2] \quad [3.28]$$

Hence, after n eliminations, equation [3.17] becomes

$$\langle G(0)\rangle = dC(n)/dE + [-2/N(0)]\{(G0)V(n)d[Ec(n)/V(n)]/dE\} + [-2/N(0)]\{d[\ln V(n)]/dE\} \quad [3.29]$$

where

$$C(n)=[-2/N(0)]\sum_{m=1}^{k-1} dQ(m)/dE \qquad [3.30]$$

The average density of states is

$$\rho(E)=(-1/\pi)\,Im\langle G(0)\rangle \qquad [3.31]$$

In order to illustrate our results, we shall consider a vibrational problem on these lattices where each site has unit mass "m" and nearest neighbours are connected by springs of force constant V. The parameters in the TBH are related to m and V as follows

$$E-\epsilon=4V-m\omega^2 \qquad [3.32a]$$

$$E-\epsilon_c=6V-m\omega^2 \qquad [3.32b]$$

where ω^2 is the frequency squared. Figures 3.3-3.7 show our results for $\rho(\omega^2)$ vs ω^2 with different values of n (n=0,1,2,3,4). The corresponding values of p-Pc are obtained from equation [3.7] with υ=1.34 .

Figure 3.3: $\rho(\omega^2)$ vs ω^2 for n=0 and p-Pc=0.6527 in two dimensions.

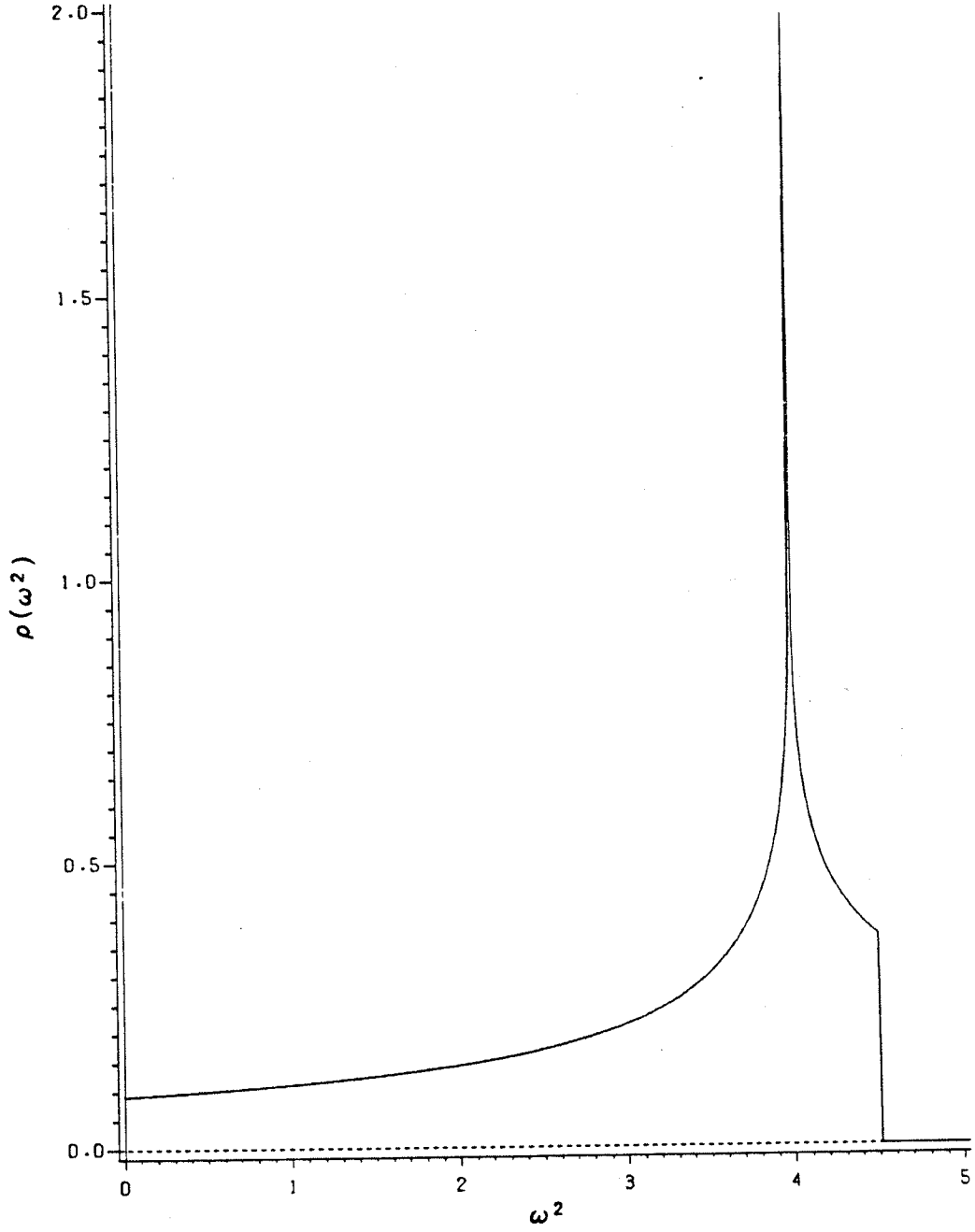

Figure 3.4: $\rho(\omega^2)$ vs ω^2 for n=1 and p-Pc=0.3891 in two dimensions.

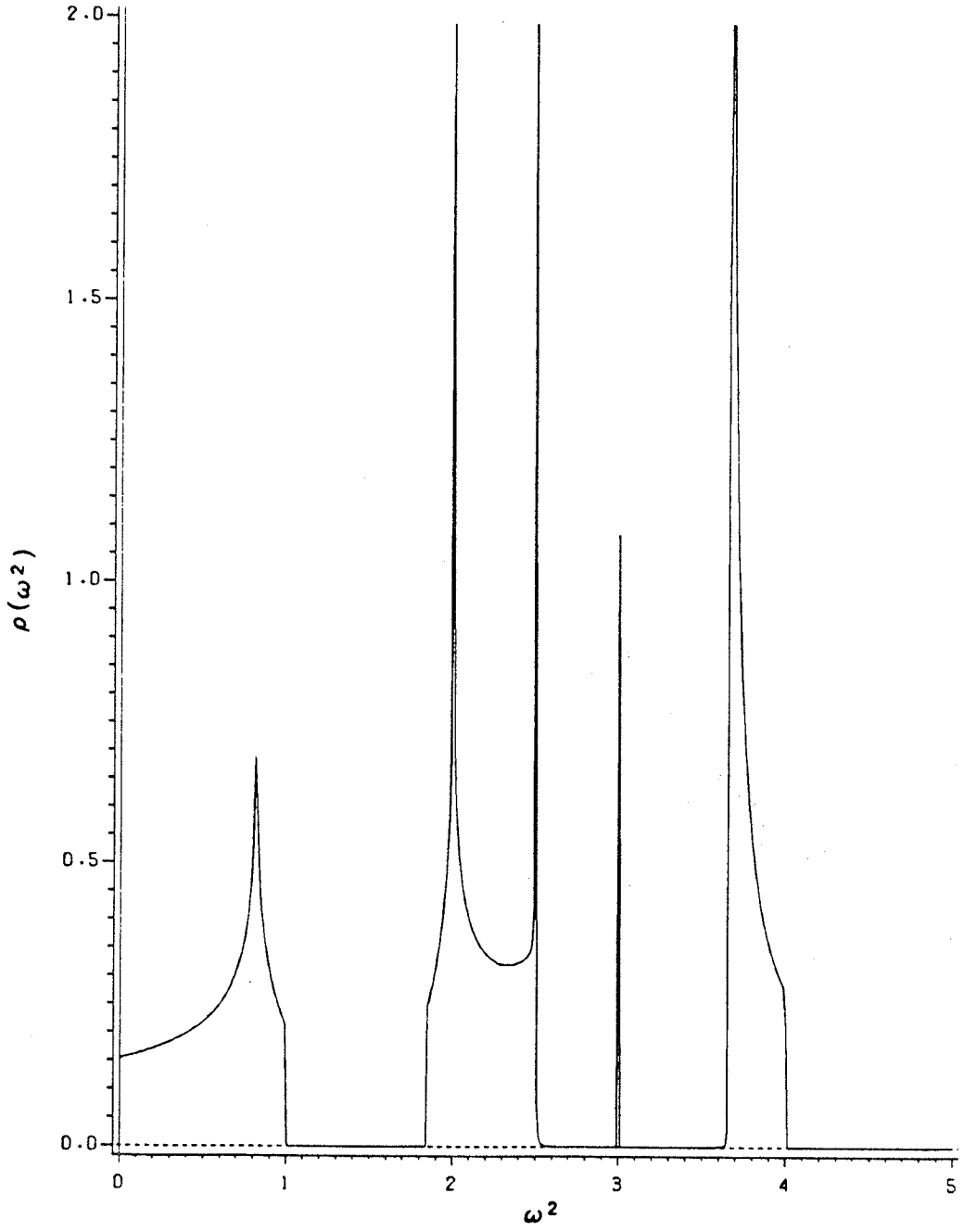

Figure 3.5: $\rho(\omega^2)$ vs ω^2 for n=2 and p-Pc=0.2320 in two dimensions.

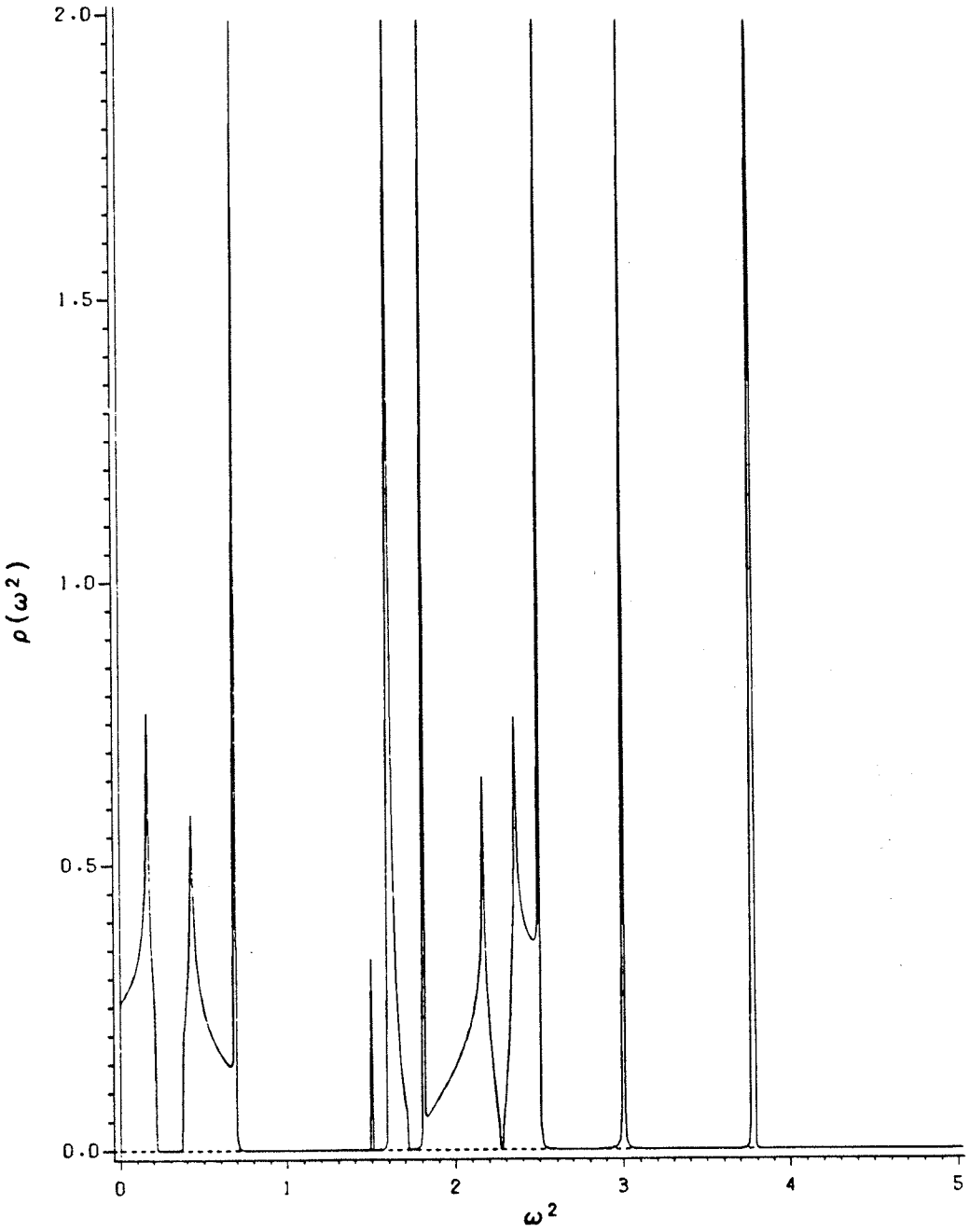

Figure 3.6: $\rho(\omega^2)$ vs ω^2 for n=3 and p-Pc=0.1383 in two dimensions.

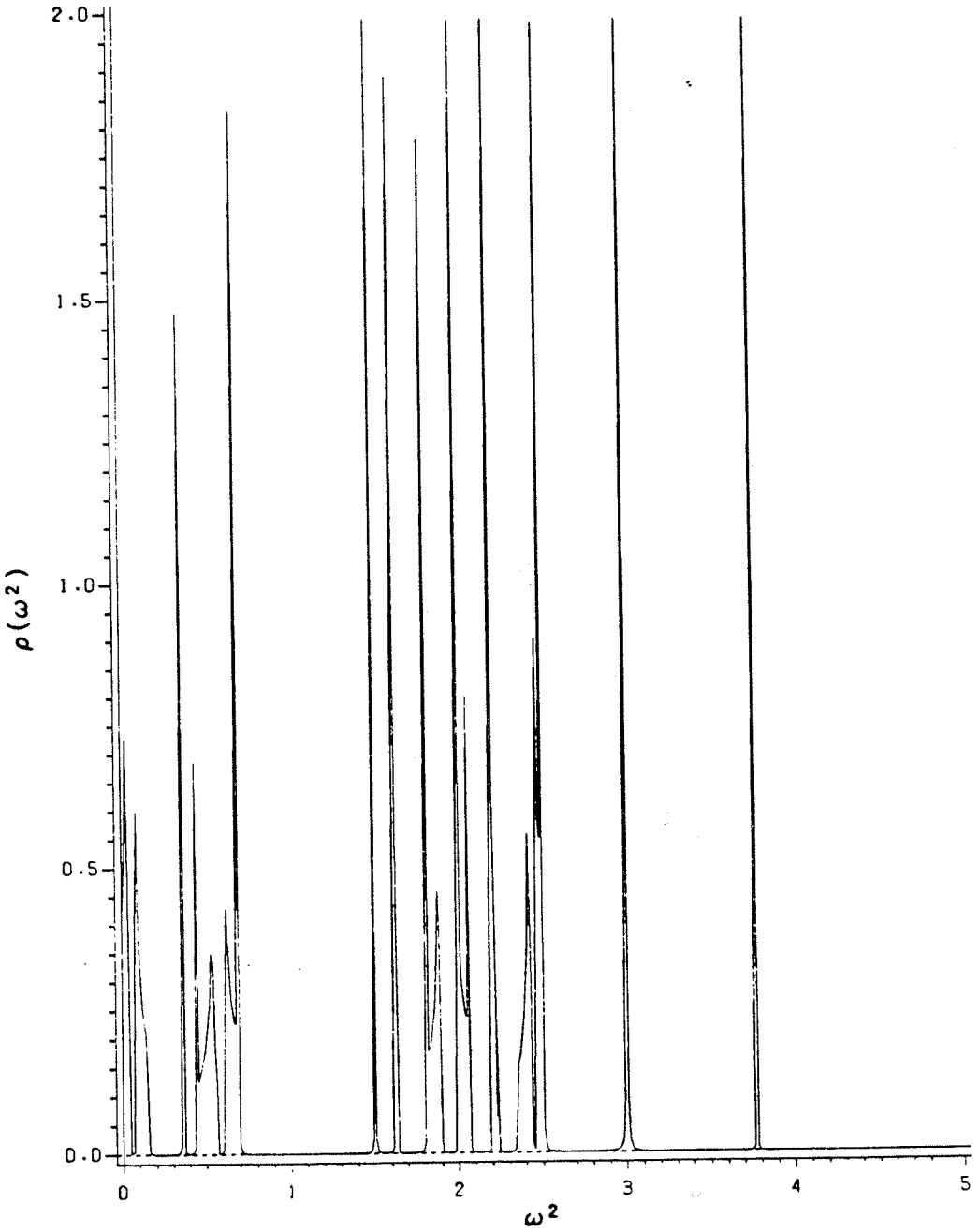

Figure 3.7: $\rho(\omega^2)$ vs ω^2 for n=4 and p-Pc=0.0824 in two dimensions.

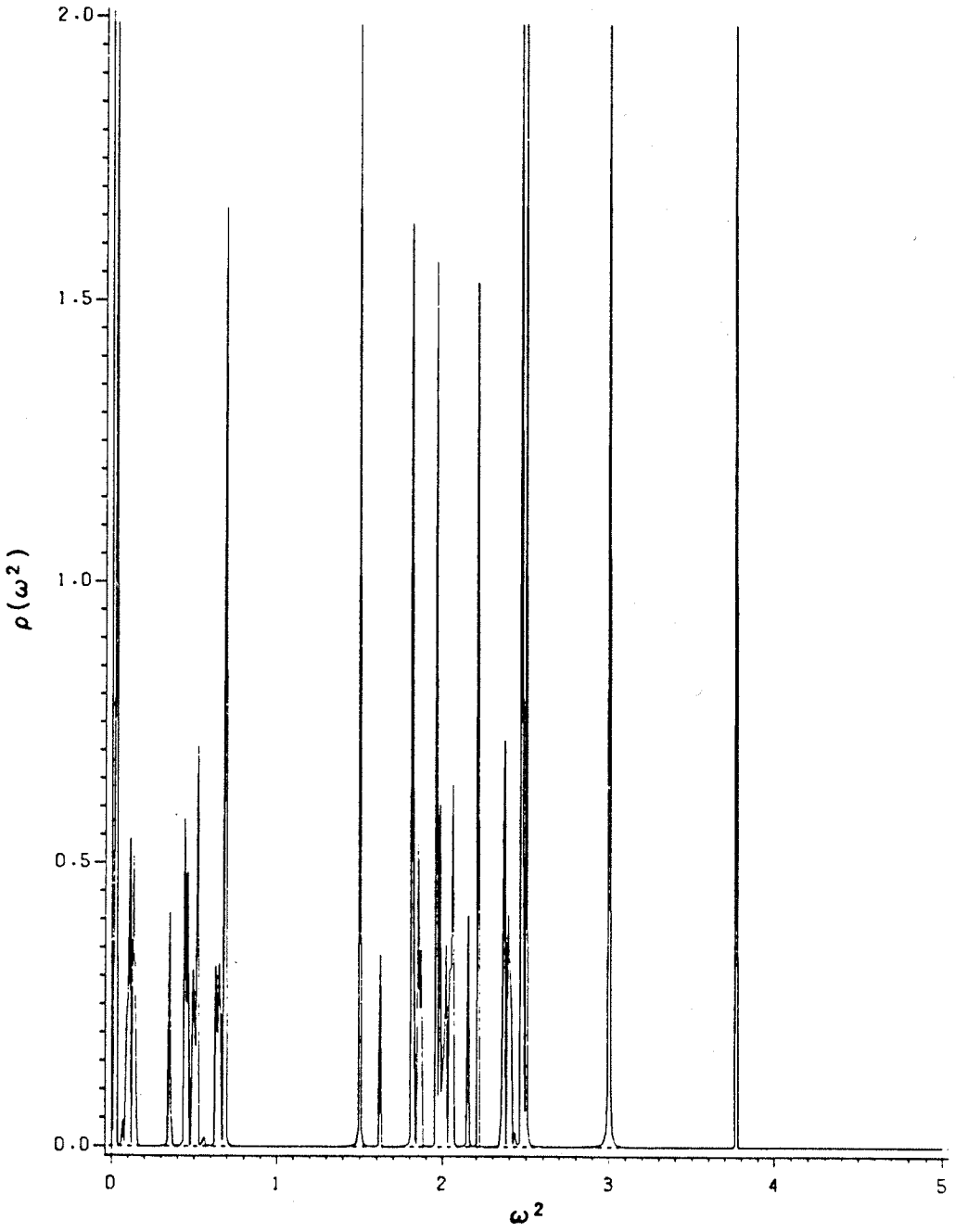

Figure 3.3 (n=0) shows the density of states for a pure triangular lattice whereas figure 3.4 (n=1) indicates the effect of adding additional sites to the "up" triangles as in figure 3.1. Notice that the spectrum has changed dramatically. It now consists of three continuous bands of energy separated by gaps and a localized vibrational mode appears in one of the gaps which is due to the absence of translational invariance in the system at small length scales. In figure 3.5 (n=2) the number of localized modes increases to three and the number of continuous bands separated by energy gaps increases to five. In general, for higher values of n (see figures 3.6 and 3.7),we observe that the number of continuous bands (and gaps) increases as does the number of localized modes. The location of these modes are fixed for each successive iteration in that a certain localized mode appearing at a particular value of n with a certain frequency ω will be present with the same frequency at higher values of n. Something that is also characteristic of these spectra is that all localized modes are below the band edge of the pure triangular lattice (n=0). In fact, for all values of n, no localized mode will appear above this band edge.

From these figures, we see that beyond a certain value of n, there is no visible change in the density of states. To observe more structure, we would have to restrict ourselves to a smaller range of energy and decrease the size of the

imaginary part in the energy. The size of the imaginary part ($1x10^{-4}$) has a lot to do in determining the structure of the density of states in that a large imaginary value tends to "smear" the spectrum by broadening the delta functions (localized modes).

For small values of n, there exists a range of frequency where the density of states has the same form as the density of states of the pure triangular lattice. For instance, at n=1 (figure 3.4), the density of states has the same structure in the range $0<\omega^2<1$ as the density of states at n=0 and for higher n values the density of states due to the triangular lattice appears in a narrower interval of frequency.

We can determine the behaviour of $\rho(\omega^2)$ at low frequencies by using the scaling relation [2.23], that is

$$\rho(\omega^2)\alpha(\omega^2)^{(d-y)/y} \qquad [3.33]$$

To determine the value of y, we must determine the fixed points of the transformation for the rescaling procedure of the pure triangular lattice as we did in section 2.1 for the one-dimensional uniform lattice. The fixed points and eigenvalues have been determined previously by Southern and Loly (1985). There is a fixed point at $\omega=0$ with eigenvalue 4 and a corresponding value of y=2. Hence $\rho(\omega^2)$ behaves at low frequencies as

$$\rho(\omega^2) \propto (\omega^2)^{d/2-1} \qquad [3.34]$$

and, in two dimensions, $\rho(\omega^2)$ is constant which is evident from figure 3.3. As n increases this low ω behaviour changes.

For length scales below ξ (i.e. n>0), the system is self-similar. At large values of n, one observes the density of states of the self-similar structure of the system which has a reduced dimensionality D. The behaviour of $\rho(\omega^2)$ at low frequencies in this case is of the form

$$\rho(\omega^2) \propto (\omega^2)^{(D-y)/y} \qquad [3.35]$$

and D=1.585 is the fractal dimension. In order to obtain the value of y we must use equation [2.24]. We must also consider the fixed points of the transformation given by equation [3.22c] and find the relevant eigenvalue. The fixed point has X=1/4 and a corresponding eigenvalue λ=5. Since we constructed our fractal lattice with a scaling factor b=2, then the exponent y has the value ln(5)/ln(2). We can write the density of states in equation [3.35] at low frequencies as follows

$$\rho(\omega^2) \propto (\omega^2)^{\tilde{D}/2-1} \qquad [3.36]$$

where D is called the spectral dimension (Rammal and Toulouse, 1983) and has the value

$$\tilde{D}=2D/y=2\ln(3)/\ln(5)=1.365 \qquad [3.37]$$

Hence our disordered structure is characterized by three different dimensionalities: d (Euclidean dimension), D (fractal dimension) and $\tilde{D}$ (spectral dimension). In a regular ordered system, these three all have the same value. In a disordered system, they obey the inequality $\tilde{D}\leq D\leq d$. Since the low temperature thermodynamic properties are determined by the spectral dimension D and not the Euclidean dimension d, we expect a crossover behaviour to occur as a function of p-Pc. The figures 3.3- 3.7 for each value of p-Pc indicate two basic regions of frequency. There is a low frequency phonon region (Euclidean) that shrinks to zero as we approach Pc ($n\rightarrow\infty$) and a higher frequency region which contains many gaps and localized modes. Alexander and Orbach (1982) have coined this higher region the "fracton" regime since it is dominated by the length scales below ξ. One would expect that for each value of n (or equivalently p-Pc) there might be a sharp crossover frequency ω_c which would separate these two regions. In fact Derrida et al (1984) have used an effective medium approximation to calculate the spectral properties of a disordered medium and found a sharp crossover frequency in both two and three

dimensions. Our results do not exhibit any sharp frequency crossover behaviour at fixed p-Pc.

Another way to study this question of a crossover frequency is to consider the integrated density of states in equation [2.42] since $N(\omega^2)$ behaves more smoothly than $\rho(\omega^2)$. Results of $N(\omega^2)$ vs (ω^2) are given in figures 3.8-3.12. For n=0, the integrated density of states is simply that of the pure lattice. At low frequencies the integrated density of states for phonons behaves as

$$N(\omega^2) \propto (\omega^2)^{d/2} \qquad [3.38]$$

where d is the Euclidean dimension. As we approach quite close to Pc (n>5), there is no further noticeable change in $N(\omega^2)$. In this limit, $N(\omega^2)$ behaves as

$$N(\omega^2) \propto (\omega^2)^{D/2} \qquad [3.39]$$

When figures 3.8-3.12 are plotted on a log-log scale, the initial slope is (d/2)=1 for small n as expected whereas for higher values of n, the slope approaches (D/2)=0.7870. Thus there is an apparent decrease in slope as we approach Pc and the amount of fractal structure in the lattice increases.

Figure 3.8: $N(\omega^2)$ vs ω^2 for n=0 and p-Pc=0.6527 in two dimensions.

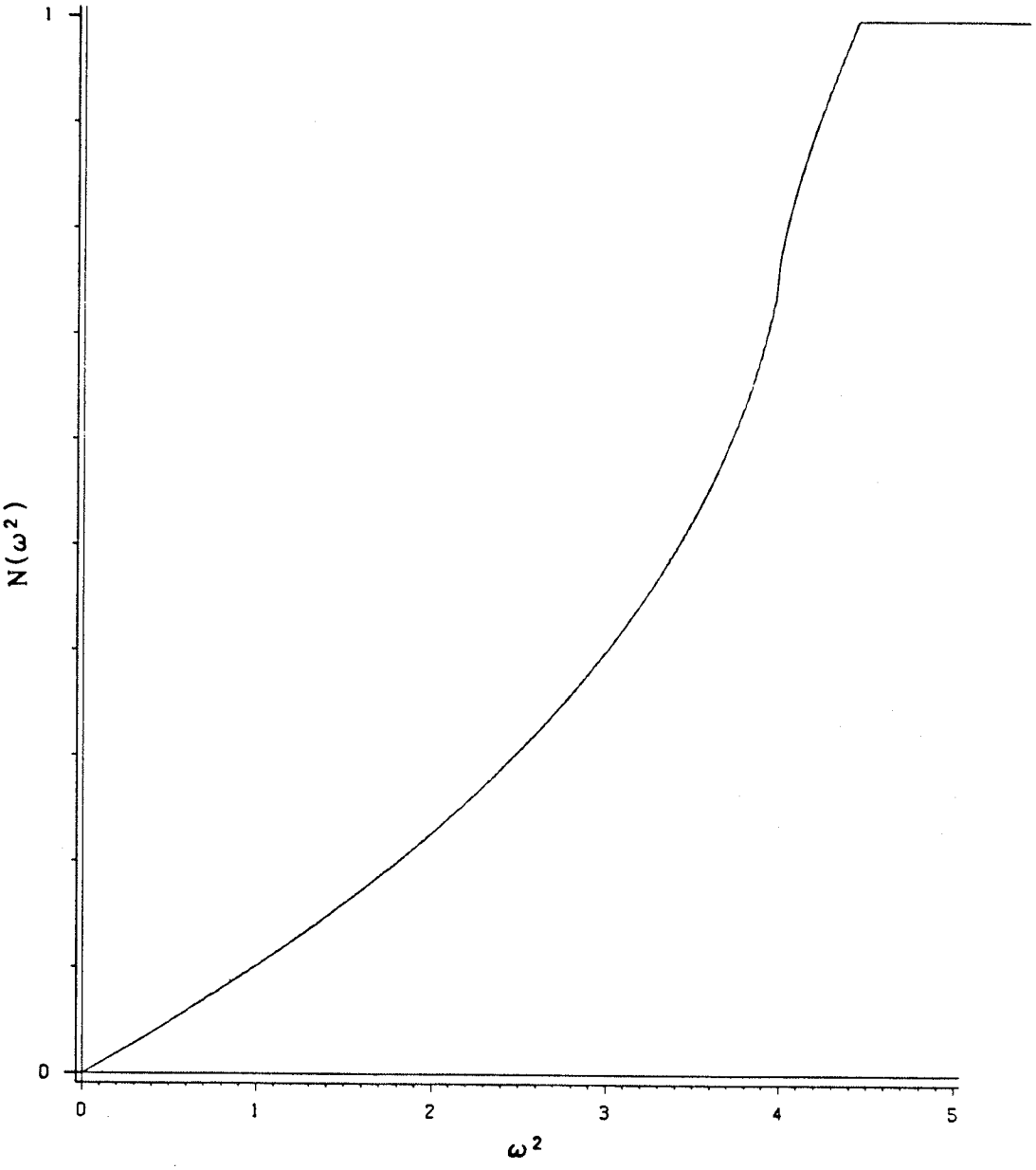

Figure 3.9: $N(\omega^2)$ vs ω^2 for n=1 and p-Pc=0.3891 in two dimensions.

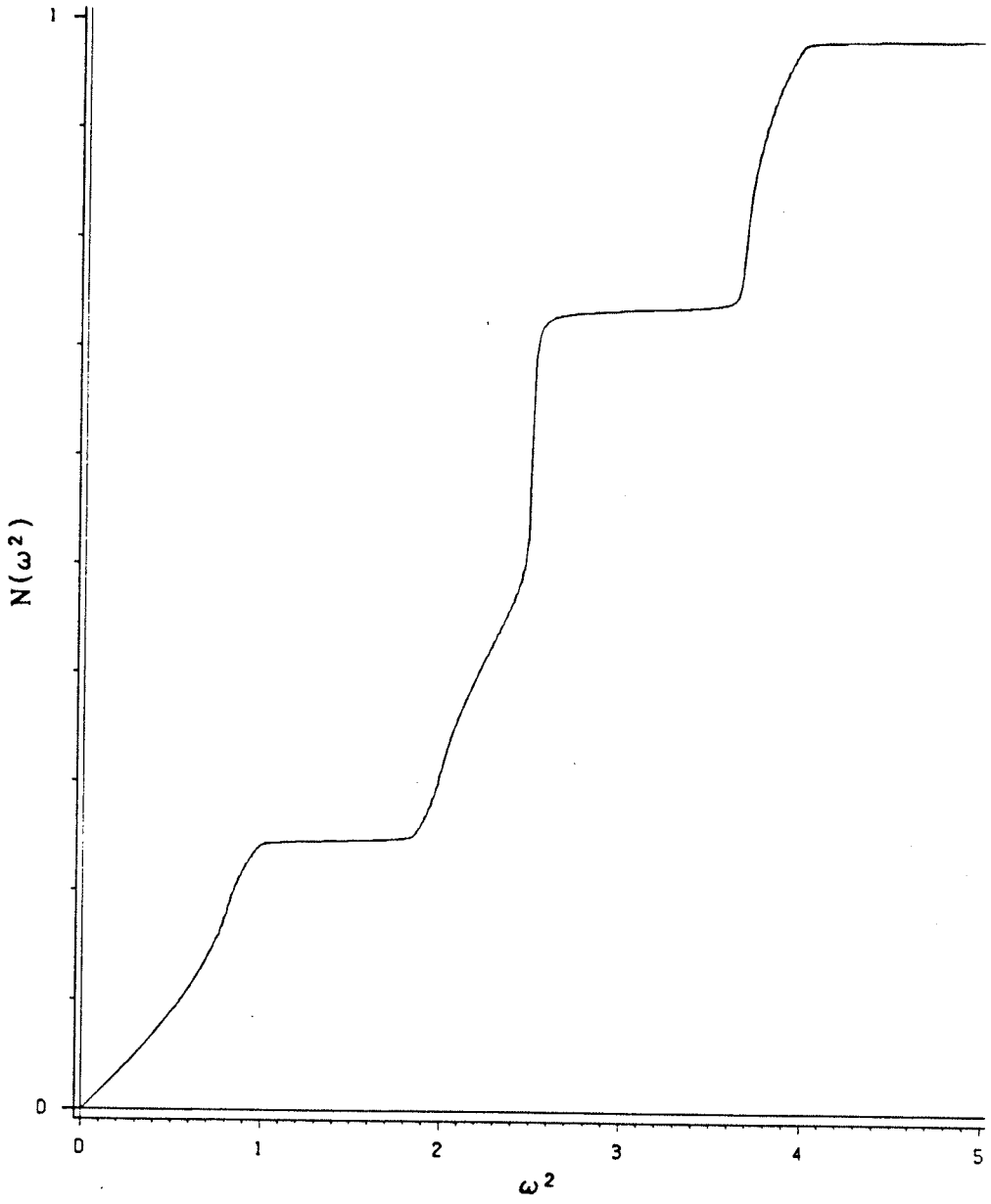

Figure 3.10: $N(\omega^2)$ vs ω^2 for n=2 and p-Pc=0.2320 in two dimensions.

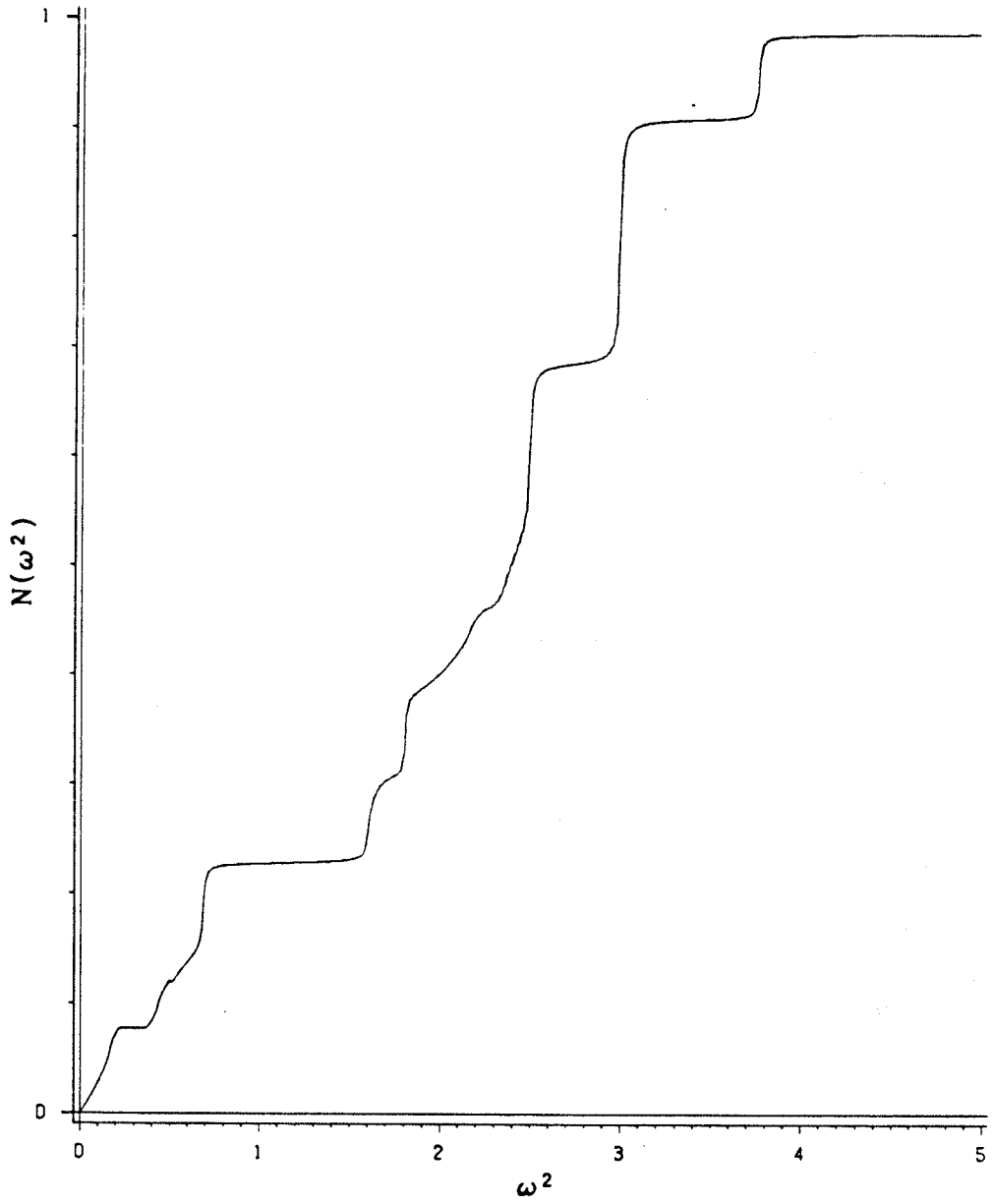

Figure 3.11: $N(\omega^2)$ vs ω^2 for n=3 and p-Pc=0.1383 in two dimensions.

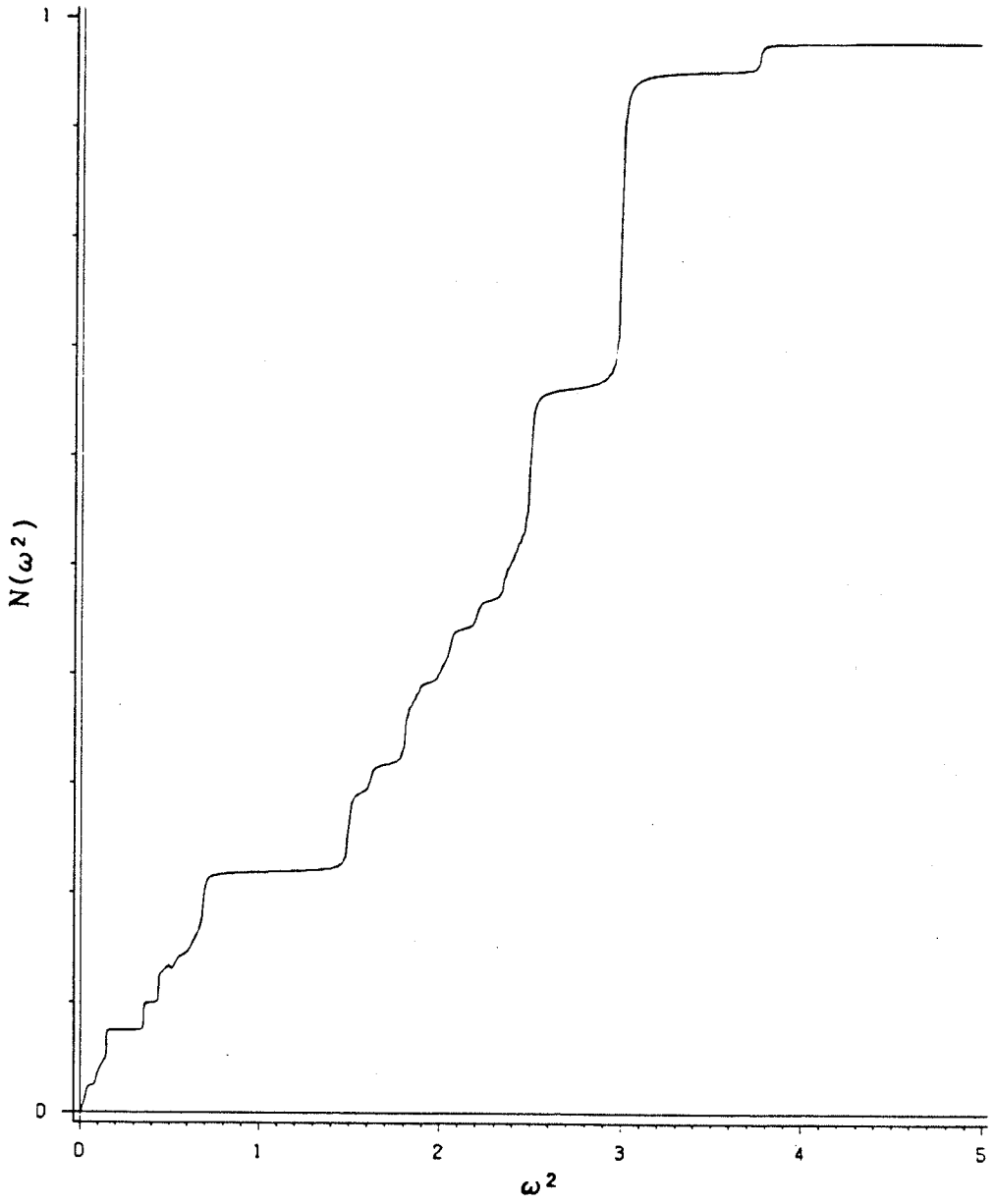

Figure 3.12: $N(\omega^2)$ vs ω^2 for n=4 and p-Pc=0.0824 in two dimensions.

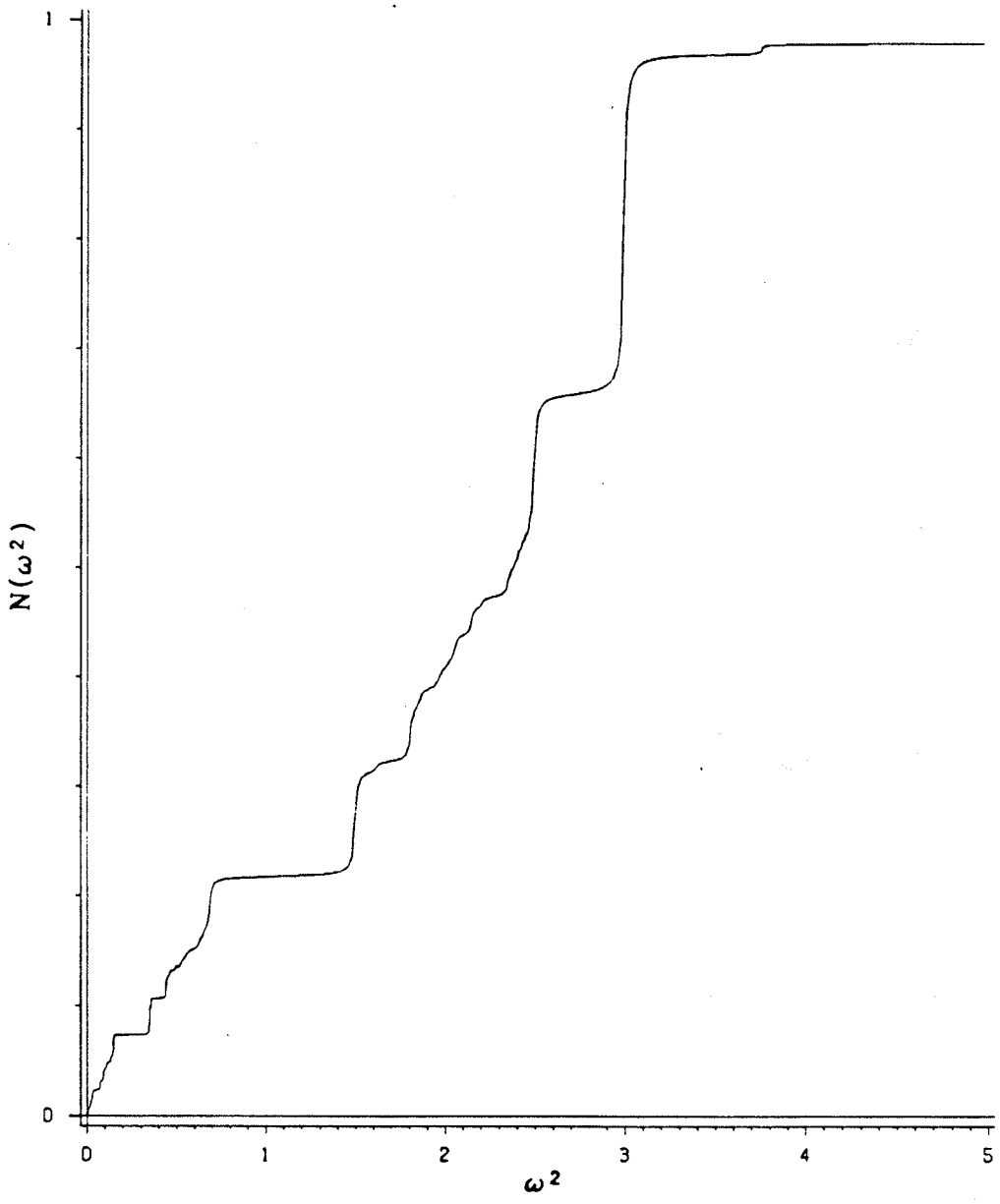

Our results for $N(\omega^2)$ for n>5 agree exactly with the results by Rammal (1984) who calculated the integrated density of states for the Sierpinski gasket analytically. Figure 3.13 shows the integrated density of states at Pc (n=oo). The discontinuous jumps in $N(\omega^2)$ are due to the localized modes in the system. We could identify the crossover frequency ω_c as being the frequency of the upper band edge of the first continuous band in the low frequency (Euclidean) region. The value of the frequency ω_c identified in this way decreases when we decrease p-Pc as shown in figure 3.14. Derrida et al (1984) predicted, using an effective medium approximation (EMA), that the crossover frequency varies linearly with p-Pc. We found that the behaviour as we approach Pc is governed by the fixed point at $\omega_c=0$. Since this fixed point has a relevant eigenvalue with a corresponding exponent y which indicates how ω^2 scales with changes in length scale, one finds that

$$\omega_c^2 \propto (a/\xi)^{y} \qquad [3.40a]$$

where y=ln(5)/ln(2). Using equation [3.6], we find that

$$\omega_c^2 \propto (p-Pc)^{\upsilon y} \qquad [3.40b]$$

where the exponent υy has the value 3.11 for d=2.

Figure 3.13: $N(\omega^2)$ vs ω^2 for $n=\infty$ and p-Pc=0.0 in two dimensions.

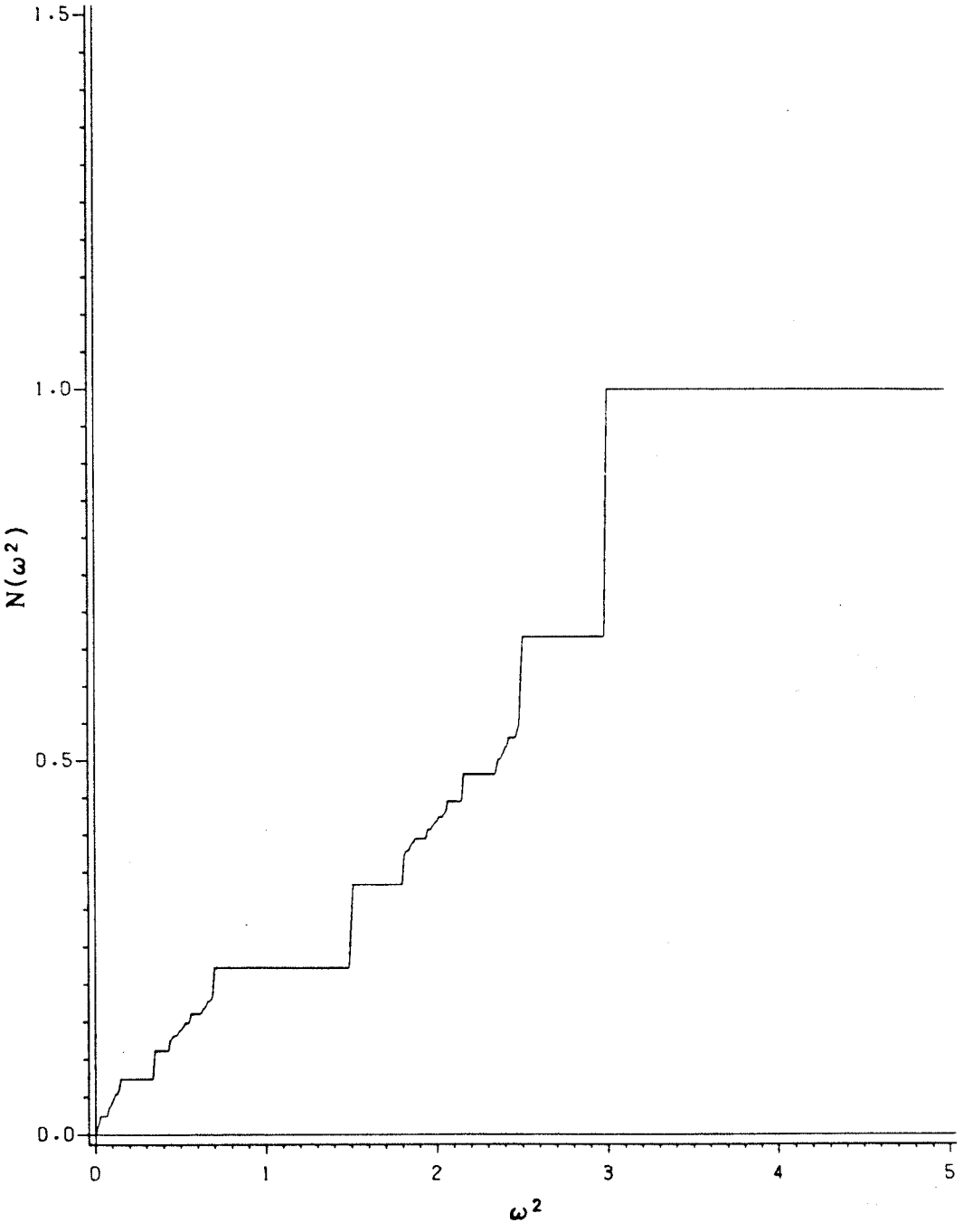

Figure 3.14: A plot of $\log(\omega_c^2)$ vs $\log(p-Pc)$ is given below. The slope of the line corresponds to the value $\upsilon y=3.11$ in two dimensions.

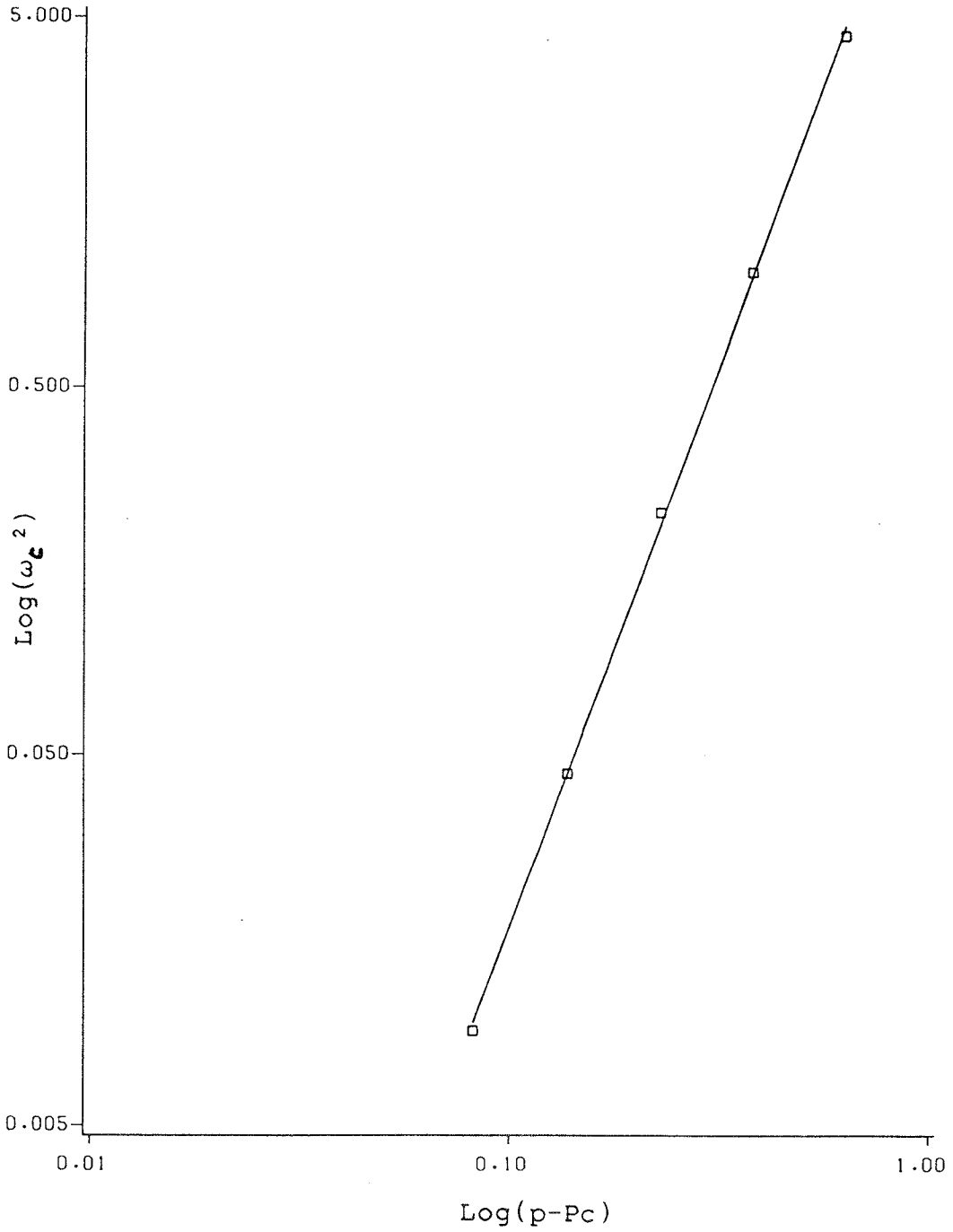

3.2 3-D FACE CENTERED CUBIC LATTICE

The treatment of the three dimensional case is identical to the two dimensional case and we will simply state the results. In two-dimensions, we took a triangular lattice and embedded fractal structure in all triangles pointing up. In three dimensions we can stack tetrahedra pointing up and pointing down such that their corner sites form a face centered cubic (FCC) lattice. Then, as for the tetrahedron in figure 2.6, we embed fractal structure into all tetrahedra pointing up. From this arrangement, we obtain the essential geometrical features of three dimensional disordered lattices that are encountered in the study of percolation clusters. Equations [3.1]- [3.17] are still applicable and using figure 3.15, the matrix form of zI-H for each tetrahedron is

$$zI-H=\begin{bmatrix} z-\epsilon & 0 & 0 & 0 & -V & 0 & 0 & -V & -V & 0 \\ 0 & z-\epsilon & 0 & 0 & -V & -V & -V & 0 & 0 & 0 \\ 0 & 0 & z-\epsilon & 0 & 0 & -V & 0 & 0 & -V & -V \\ 0 & 0 & 0 & z-\epsilon & 0 & 0 & -V & -V & 0 & -V \\ -V & -V & 0 & 0 & z-\epsilon & -V & -V & -V & -V & 0 \\ 0 & -V & -V & 0 & -V & z-\epsilon & -V & 0 & -V & -V \\ 0 & -V & 0 & -V & -V & -V & z-\epsilon & -V & 0 & -V \\ -V & 0 & 0 & -V & -V & 0 & -V & z-\epsilon & -V & -V \\ -V & 0 & -V & 0 & -V & -V & 0 & -V & z-\epsilon & -V \\ 0 & 0 & -V & -V & 0 & -V & -V & -V & -V & z-\epsilon \end{bmatrix} \qquad [3.41]$$

Figure 3.15:
a) This is a block used to obtain the matrix elements of zI-H.
b) The same block after sites have been eliminated.

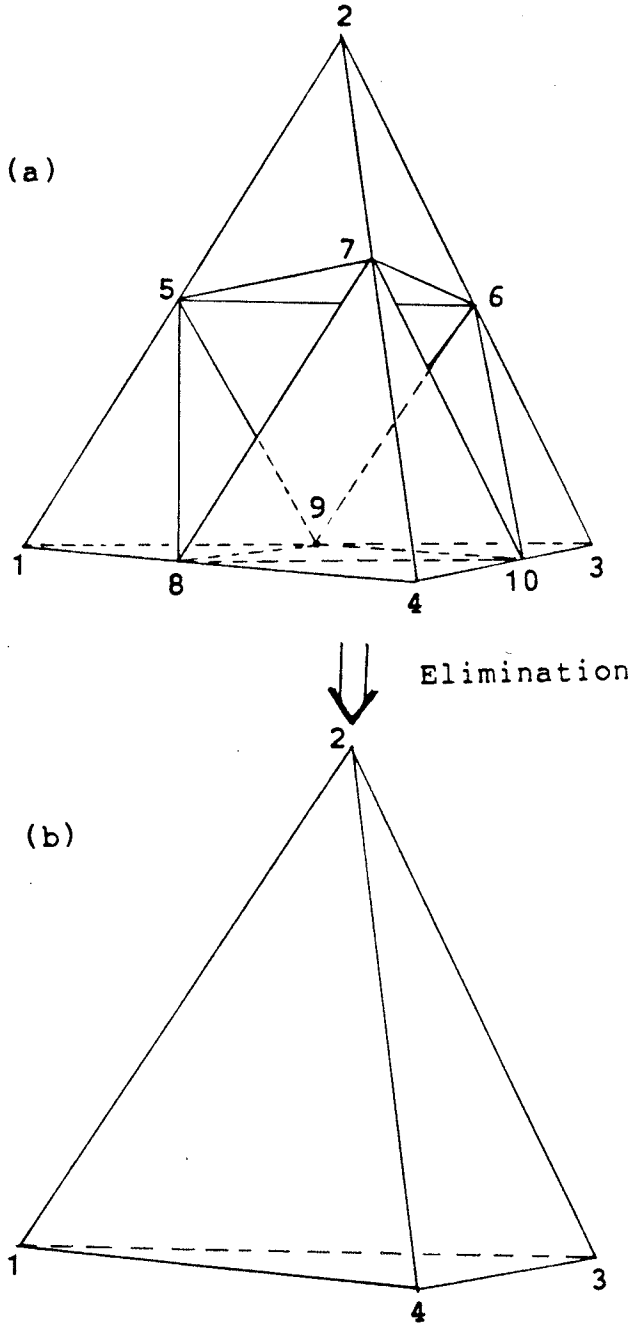

The sites (1,2,3,4) in figure 3.15 will interact with another block of six not shown in the diagram (N_b =6), however, as in two dimensions, we need only multiply the renormalized energy parameter by a factor (q=2). We eliminate sites 5,...,10 to determine new effective parameters for the remaining sites. Hence we partition the matrix H in the following way

$$H_{11}=\begin{bmatrix}\epsilon & 0 & 0 & 0\\ 0 & \epsilon & 0 & 0\\ 0 & 0 & \epsilon & 0\\ 0 & 0 & 0 & \epsilon\end{bmatrix}$$

$$H_{12}=\begin{bmatrix}V & 0 & 0 & V & V & 0\\ V & V & V & 0 & 0 & 0\\ 0 & V & 0 & 0 & V & V\\ 0 & 0 & V & V & 0 & V\end{bmatrix}$$

[3.42]

$$H_{21}=\begin{bmatrix}V & V & 0 & 0\\ 0 & V & V & 0\\ 0 & V & 0 & V\\ V & 0 & 0 & V\\ V & 0 & V & 0\\ 0 & 0 & V & V\end{bmatrix}$$

$$H_{22}=\begin{bmatrix} \epsilon & V & V & V & V & 0 \\ V & \epsilon & V & 0 & V & V \\ V & V & \epsilon & V & 0 & V \\ V & 0 & V & \epsilon & V & V \\ V & V & 0 & V & \epsilon & V \\ 0 & V & V & V & V & \epsilon \end{bmatrix}.$$

and using equation [3.11], we find the following renormalized parameters with $x=V/(z-\epsilon)$

$$z-\epsilon'=(z-\epsilon)[(1+2x)(1-6x+6x^2)]/(1-4x) \qquad [3.43a]$$

$$V'=V[x(1+2x)]/(1-4x) \qquad [3.43b]$$

$$x'=x^2/(6x^2-6x+1) \qquad [3.43c]$$

$$\det(zI-H_{22})=(z-\epsilon)^6(-16x^3-12x^2+1) \qquad [3.43d]$$

where equation [3.43d] is the determinant of each block. When we consider the whole lattice, we must include another renormalized parameter as we did in two dimensions, namely

the corner site energy ϵ_c. The corner sites interact with four blocks (q_c=4) and our corner site energy is

$$z-\epsilon_c'=z-\epsilon_c - (q_c)3(z-\epsilon)x^2(2x-1)/(4x-1) \qquad [3.44]$$

and in dimensionless form [$x_c=V/(z-\epsilon_c)$], we find

$$x_c'=x(x_c)(1+2x)/[1-4x-12x(x_c)(1-2x)] \qquad [3.45]$$

Finally, if the initial disordered system has been constructed using "n" iterations of the tetrahedron on a FCC lattice with N sites, then the total number of sites after k eliminations is

$$N(k)=N[1 + 2(4^{n-k}-1)] \qquad [3.46]$$

Hence, after n eliminations our average Green's function takes on the same form as equation [3.29] except that now N(0) is given by [3.46] above and G0 is the Green function for the pure FCC lattice which has been calculated by Morita and Horiguchi (1970). In addition, the derivatives in equation [3.29] are evaluated using equations [3.43] - [3.44]. The corresponding values of p-Pc are obtained from equation [3.7] with υ=0.85 .

We now consider a vibrational problem as we did in two dimensions but the TBH parameters are related to the mass "m" and spring constant V as follows

$$E-\epsilon=6V-m\omega^2 \qquad [3.47]$$

$$E-\epsilon_c=12V-m\omega^2 \qquad [3.48]$$

Our results for $\rho(\omega^2)$ vs ω^2 with different values of n (n=0,1,2,3,4) are given in figures 3.16- 3.20. The discussion for the density of states in two dimensions concerning the continuous bands of energy, energy band gaps and localized modes is applicable to this three dimensional system. In the figures, we observe the same pattern for the phonon portion of the density of states in that it becomes compressed as n increases. For low n, we expect the density of states to behave as follows

$$\rho(\omega^2)\alpha(\omega^2)^{d/y-1} \qquad [3.49]$$

where the exponent y for the pure FCC lattice has been determined using the Rescaling method by Southern and Loly (1985) and has the value y=2. For length scales below ξ (larger ω), and for higher n values, we must find the fixed

Figure 3.16: $\rho(\omega^2)$ vs ω^2 for n=0 and p-Pc=0.8010 in three dimensions

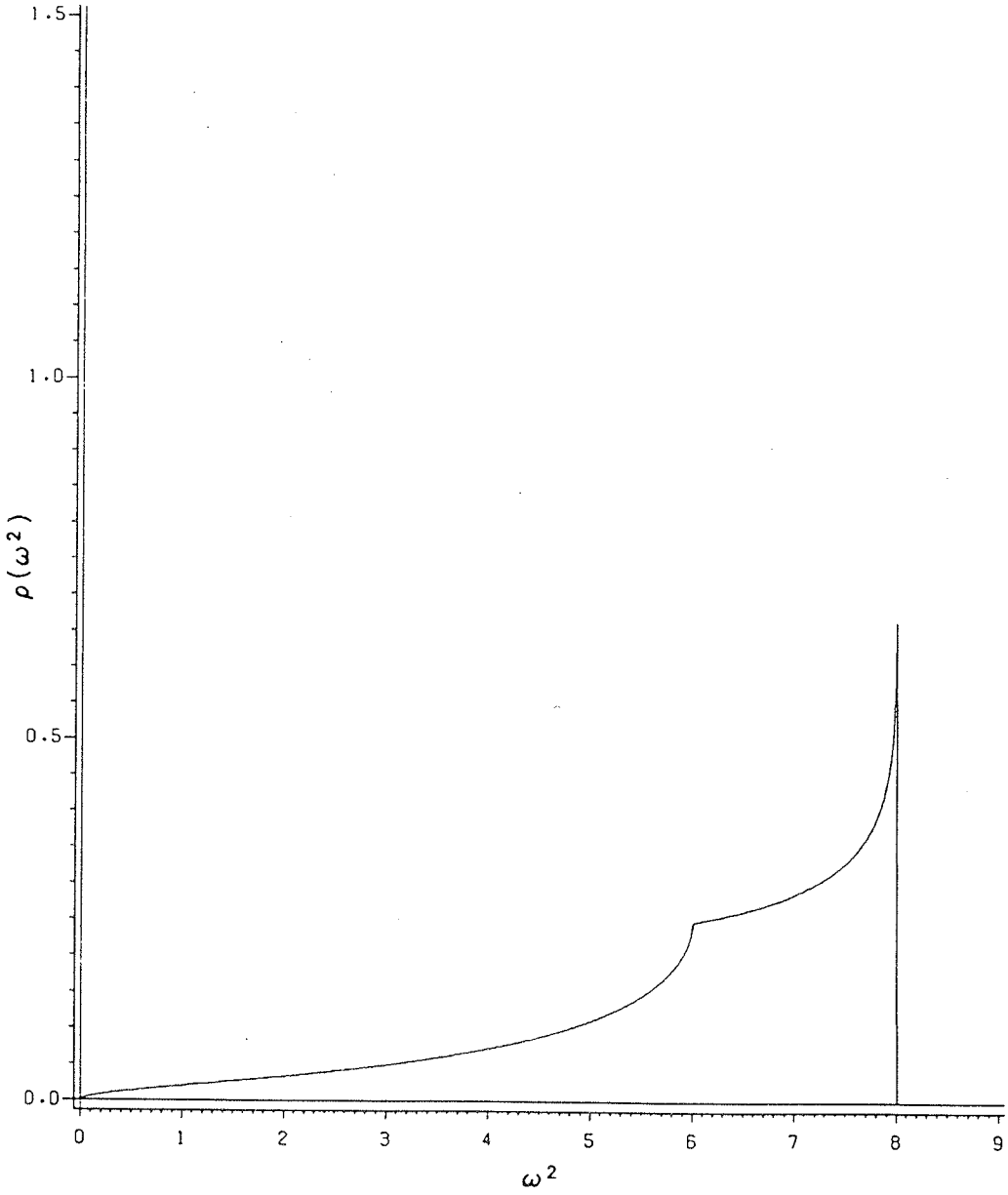

Figure 3.17: $\rho(\omega^2)$ vs ω^2 for n=1 and p-Pc=0.3544 in three dimensions

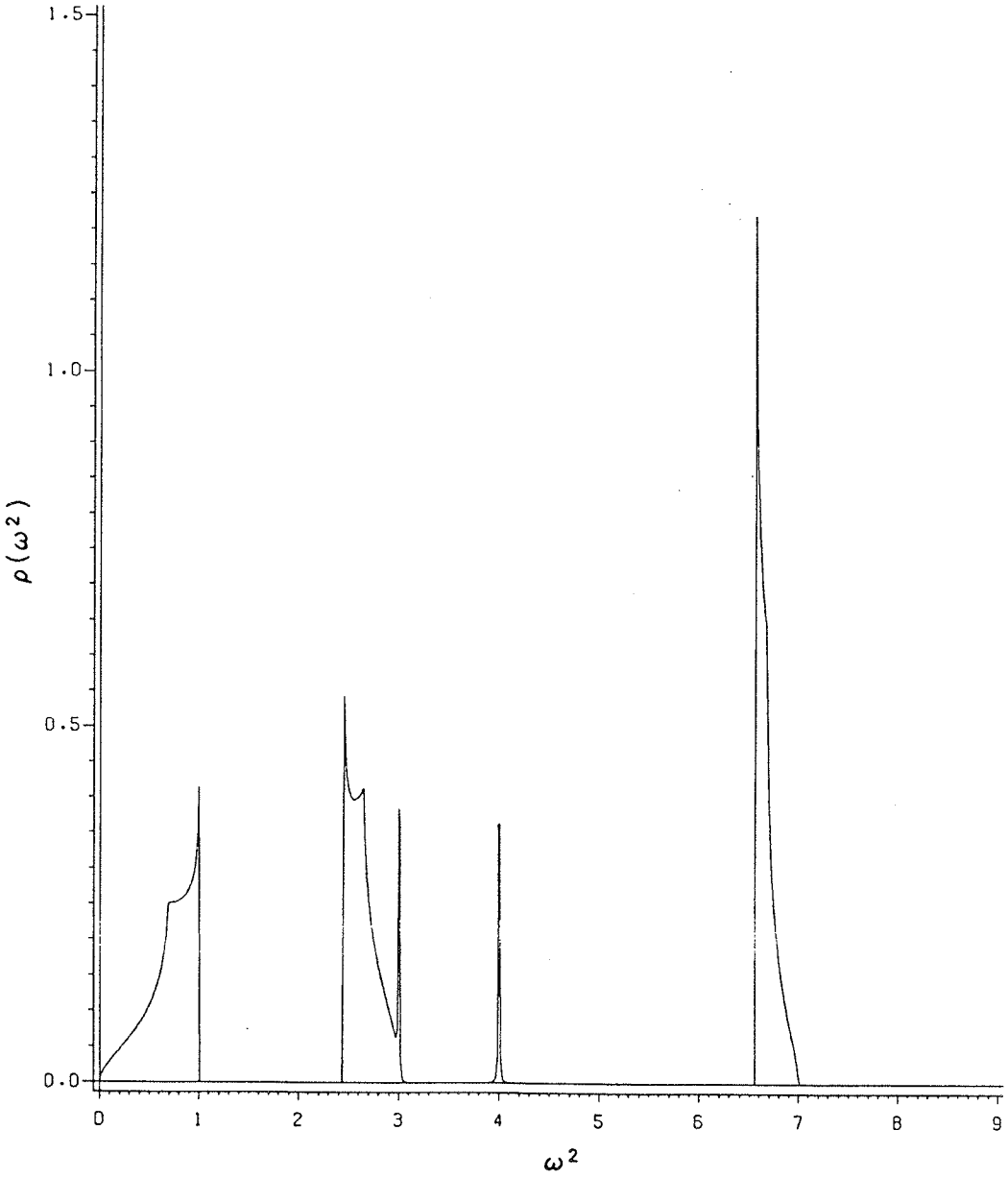

Figure 3.18: $\rho(\omega^2)$ vs ω^2 for n=2 and p-Pc=0.1508 in three dimensions

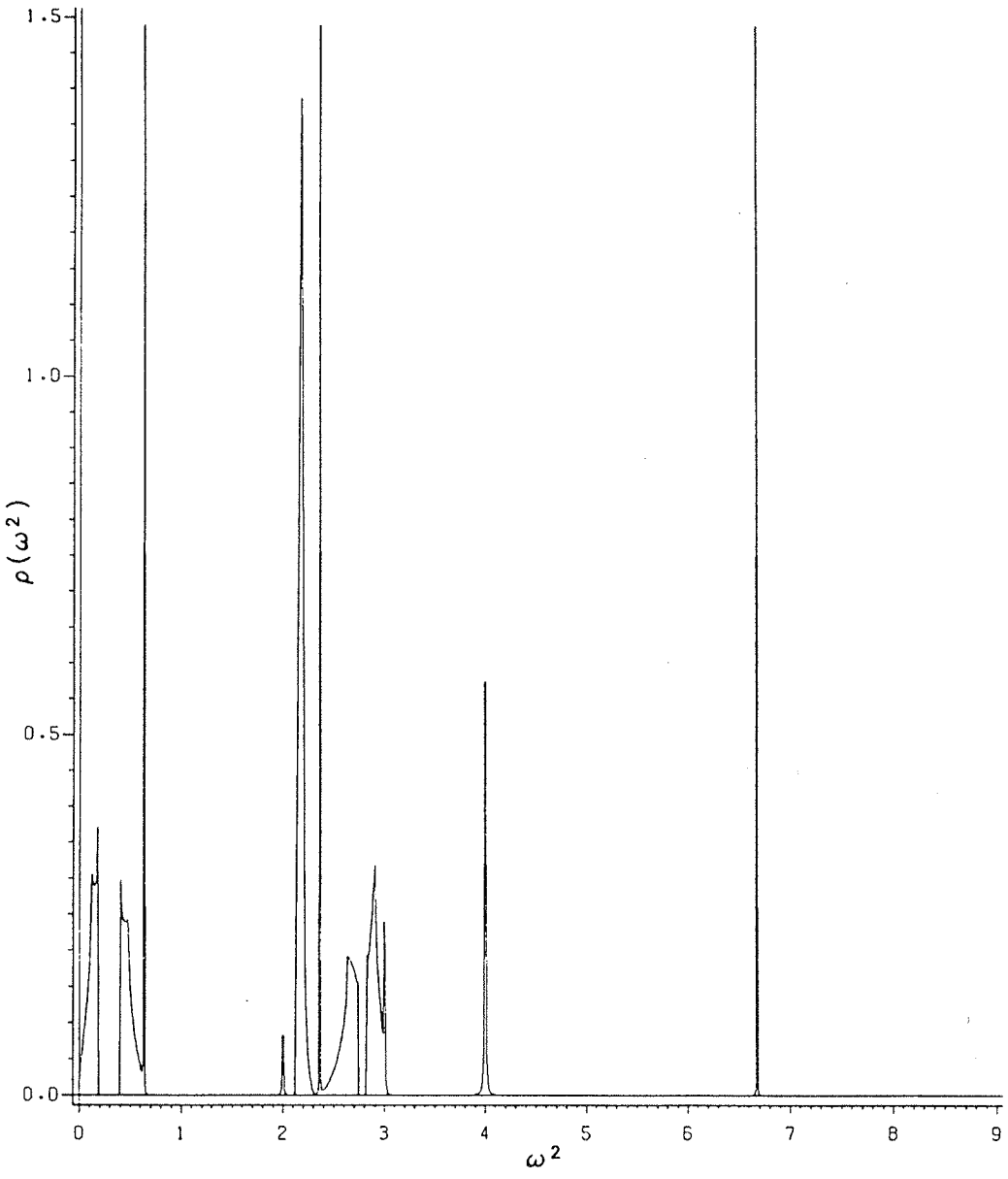

Figure 3.19: $\rho(\omega^2)$ vs ω^2 for n=3 and p-Pc=0.0694 in three dimensions

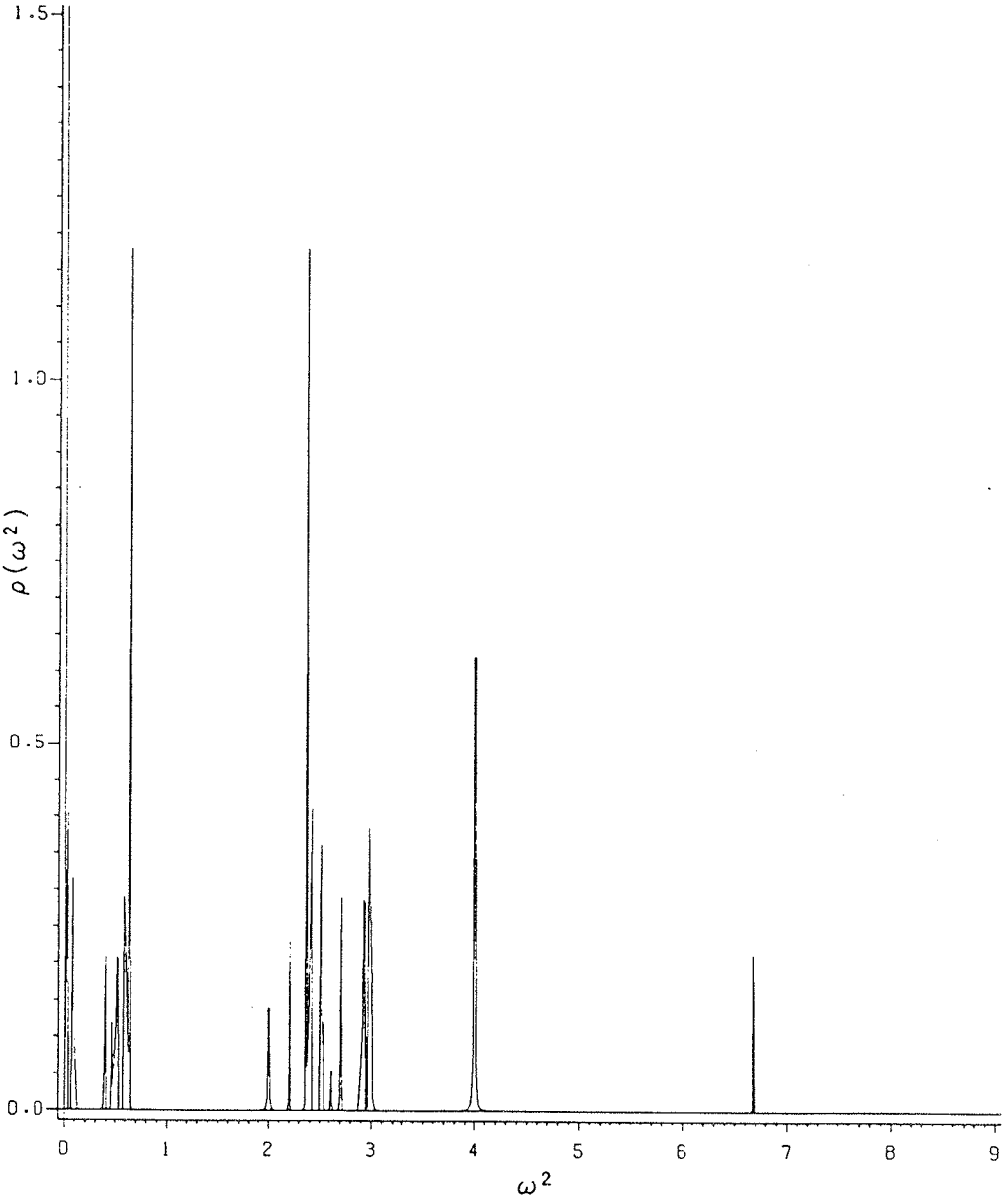

Figure 3.20: $\rho(\omega^2)$ vs ω^2 for n=4 and p-Pc=0.0307 in three dimensions

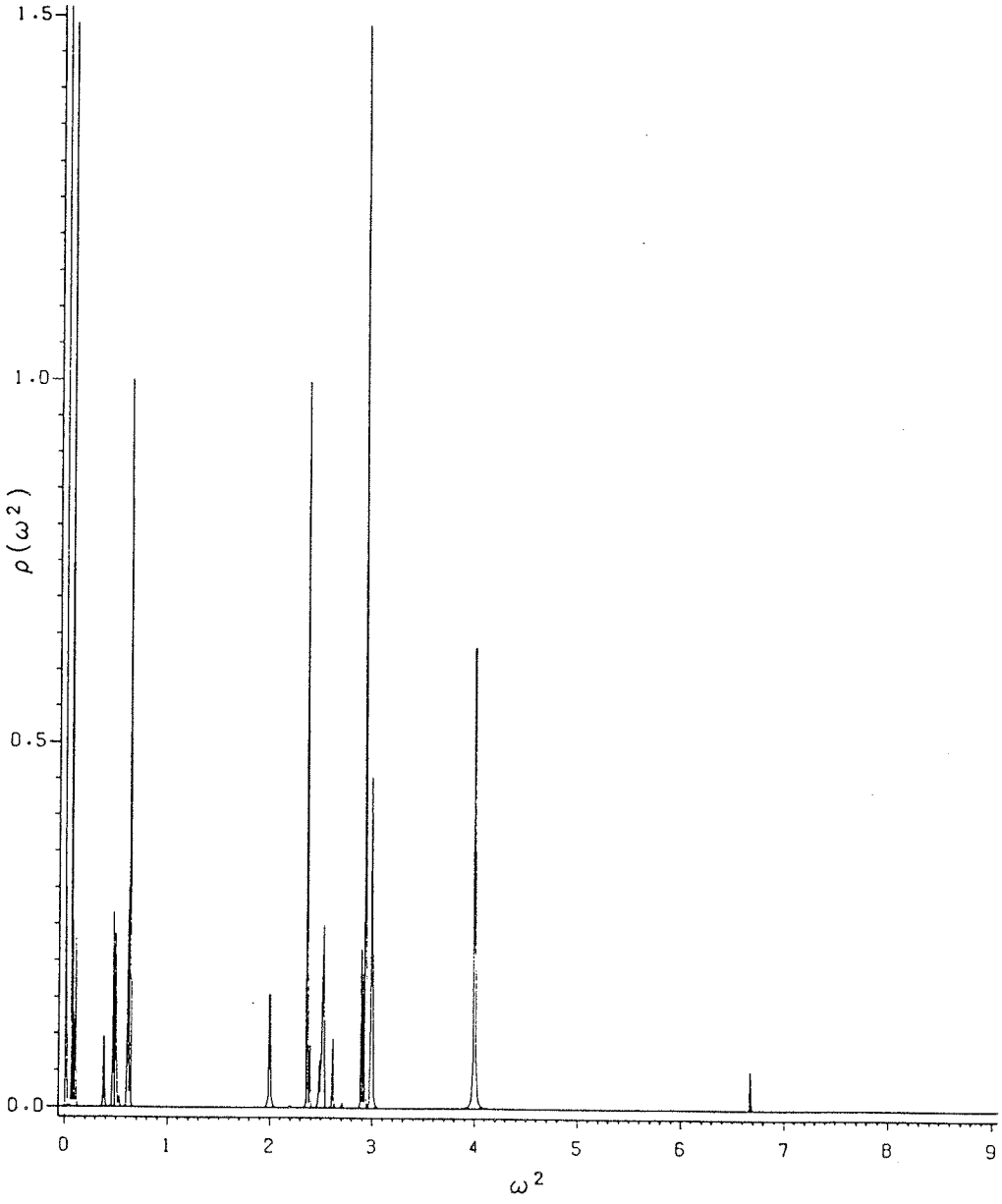

point of equation [3.43c] which gives the relevant eigenvalue of the transformation. This fixed point is X=1/6 and the corresponding eigenvalue is λ=6. From figure 3.15, it is easily seen that the scaling factor is b=2 and from equation [2.24], we find that y=ln(6)/ln(2). The spectral dimension for our system in three dimensions is then

$$\tilde{D}=2D/y=2[\ln(4)/\ln(6)]=1.547 \qquad [3.50]$$

where D has the value 2. Hence the low frequency density of states becomes enhanced as we approach Pc. Note that there is no abrupt change in $\rho(\omega^2)$ as we go from the phonon regime to the fracton regime.

The integrated density of states for different n values (n=0,1,2,3,4) is plotted in figures 3.21- 3.25 and we find that beyond n=4, $N(\omega^2)$ does not change. Figure 3.26 shows the integrated density of states at Pc ($n=\infty$). The curves for $N(\omega^2)$ that we obtained for n>5 agree exactly with the curves by Rammal (1984) who calculated $N(\omega^2)$ analytically for the hyper-tetrahedron. We can also define a crossover frequency ω_c which arbitrarily separates the phonon and fracton regions as was done in two dimensions using the integrated density of states. Figure 3.27 shows a log-log plot of ω_c^2 vs p-Pc. The slope of the line is 2.22 which corresponds to the value of υy for d=3.

Figure 3.21: $N(\omega^2)$ vs ω^2 for n=0 and p-Pc=0.8010 in three dimensions.

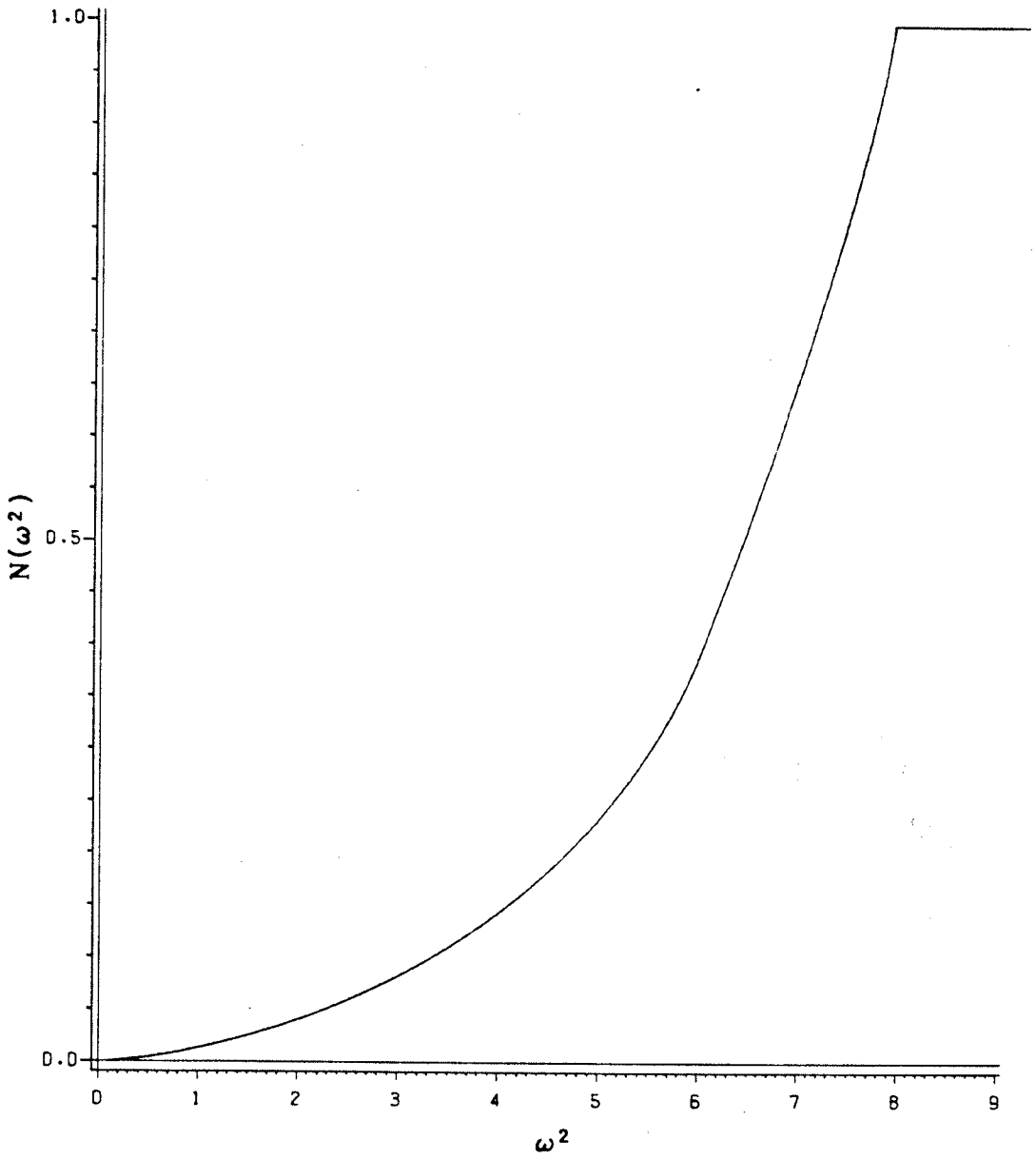

Figure 3.22: $N(\omega^2)$ vs ω^2 for n=1 and p-Pc=0.3544 in three dimensions.

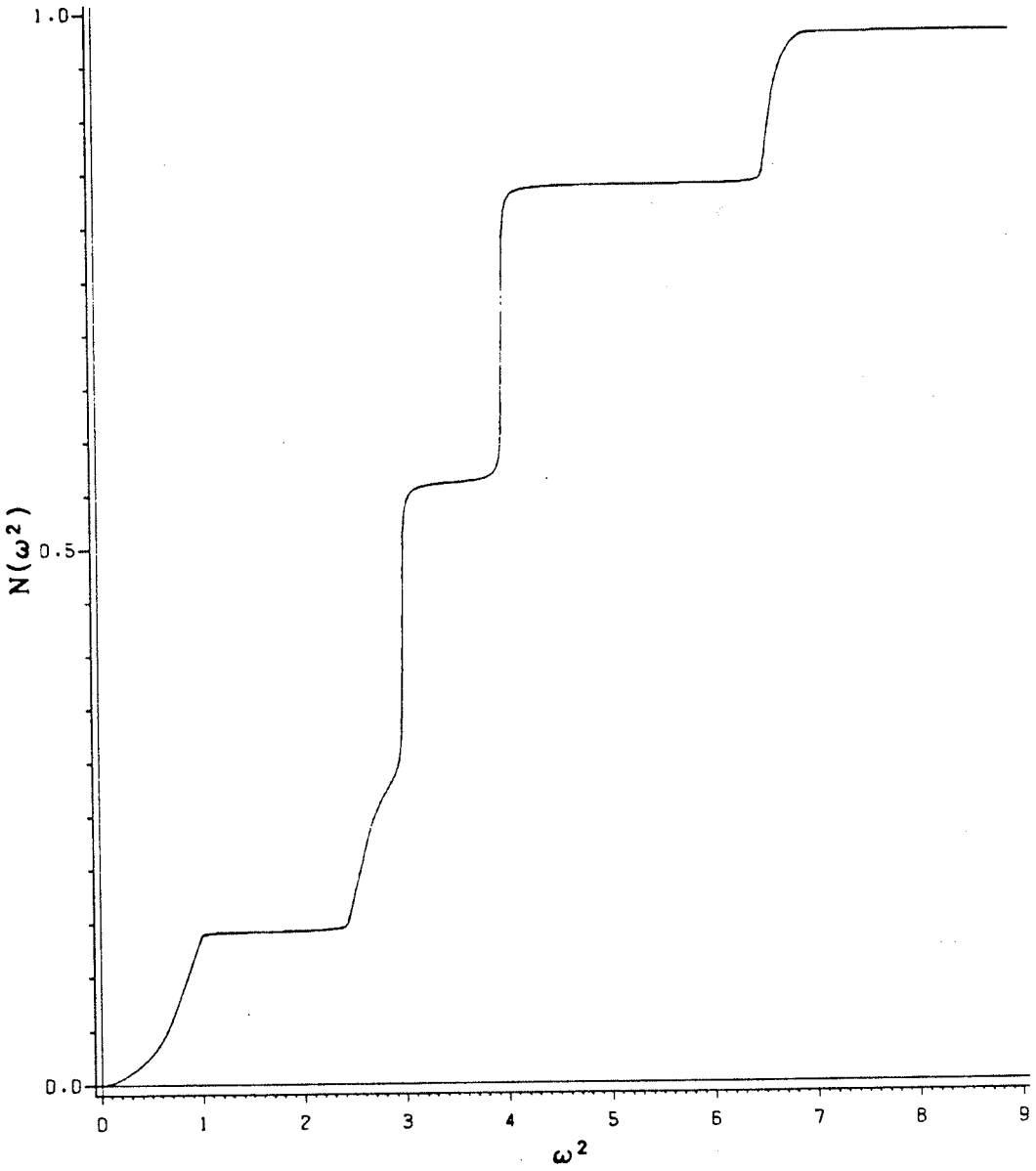

Figure 3.23: $N(\omega^2)$ vs ω^2 for n=2 and p-Pc=0.1568 in three dimensions.

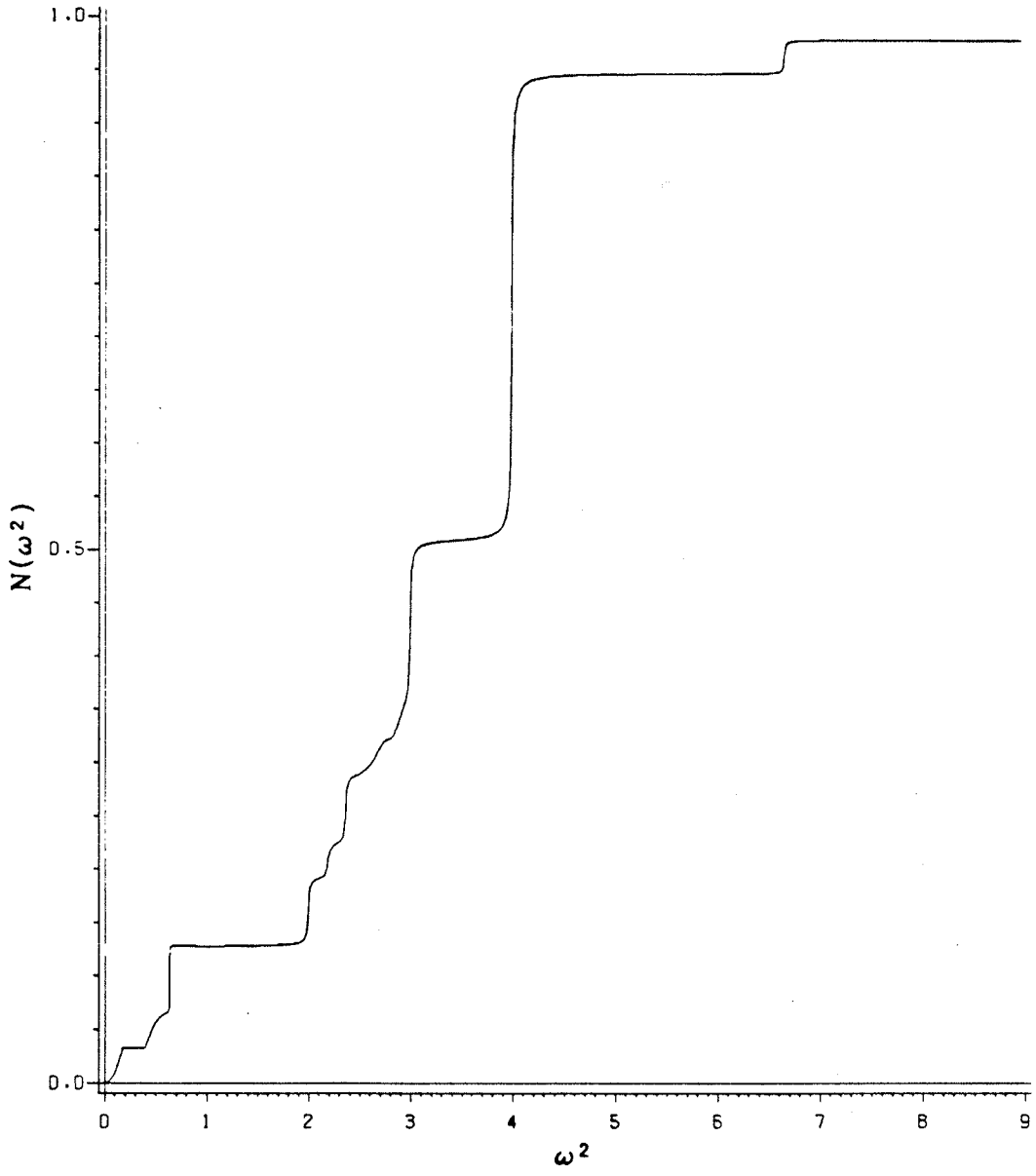

Figure 3.24: $N(\omega^2)$ vs ω^2 for n=3 and p-Pc=0.0694 in three dimensions.

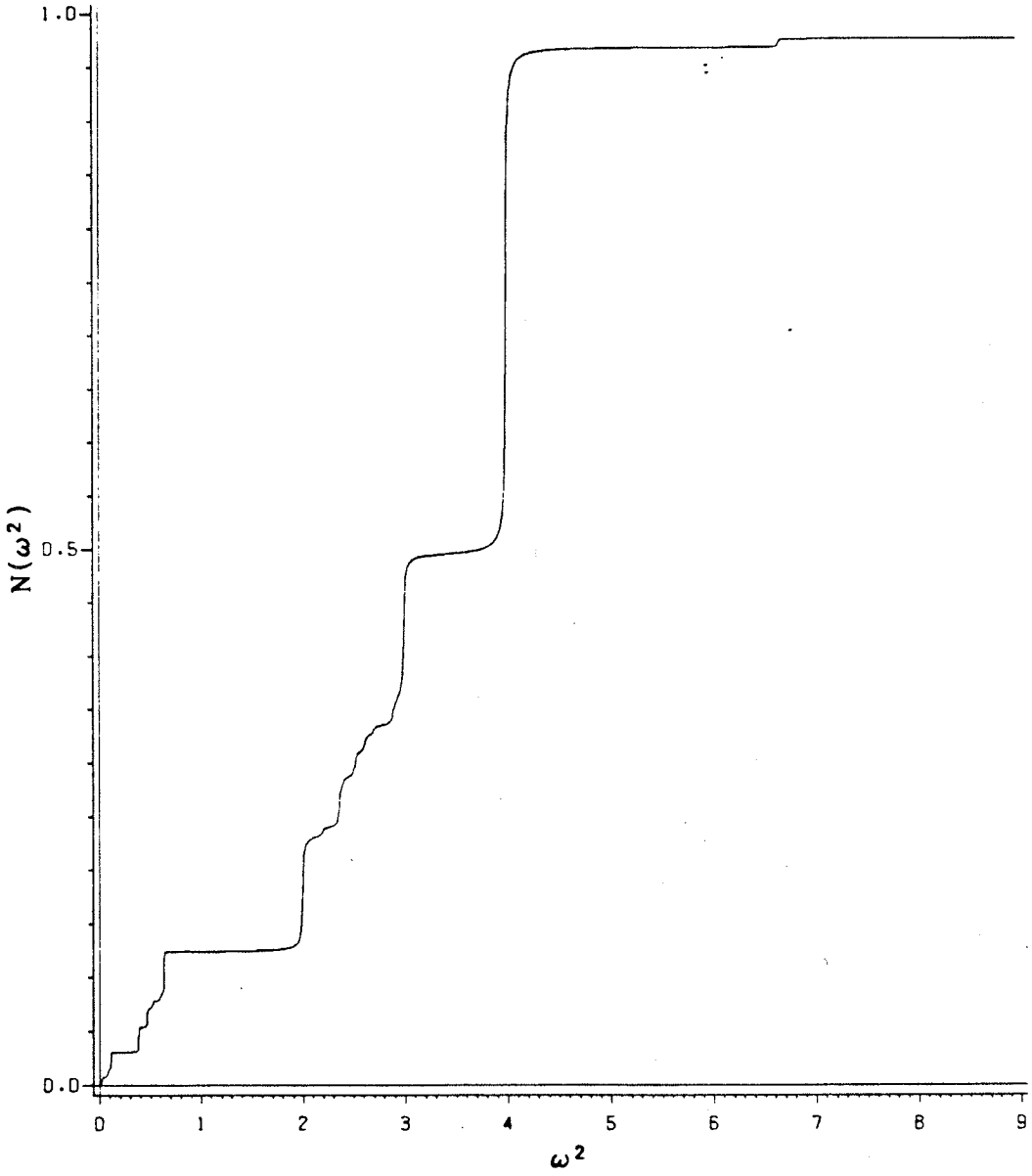

Figure 3.25: $N(\omega^2)$ vs ω^2 for n=4 and p-Pc=0.0307 in three dimensions.

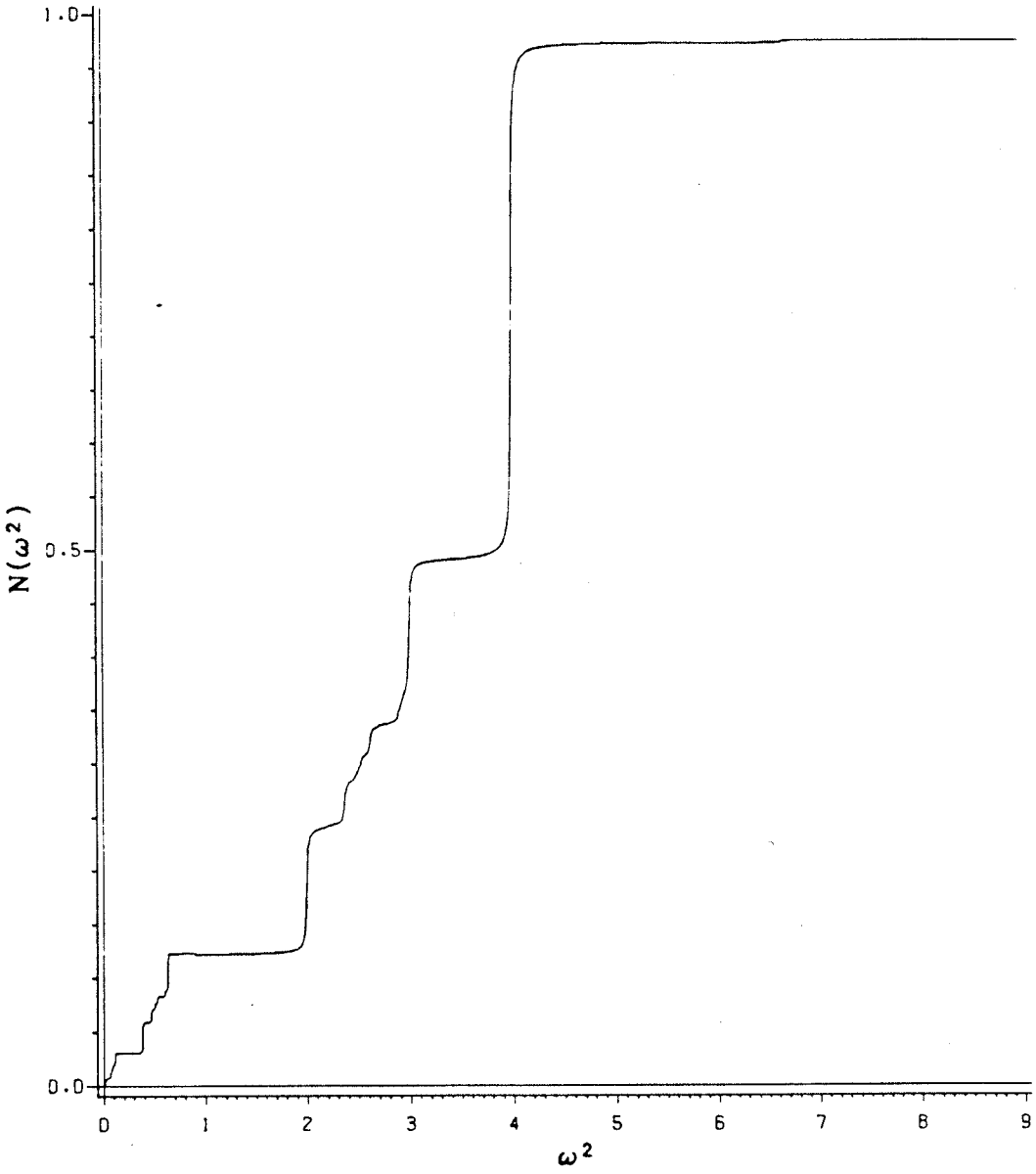

Figure 3.26: $N(\omega^2)$ vs ω^2 for $n=\infty$ and $p-Pc=0.0$ in three dimensions.

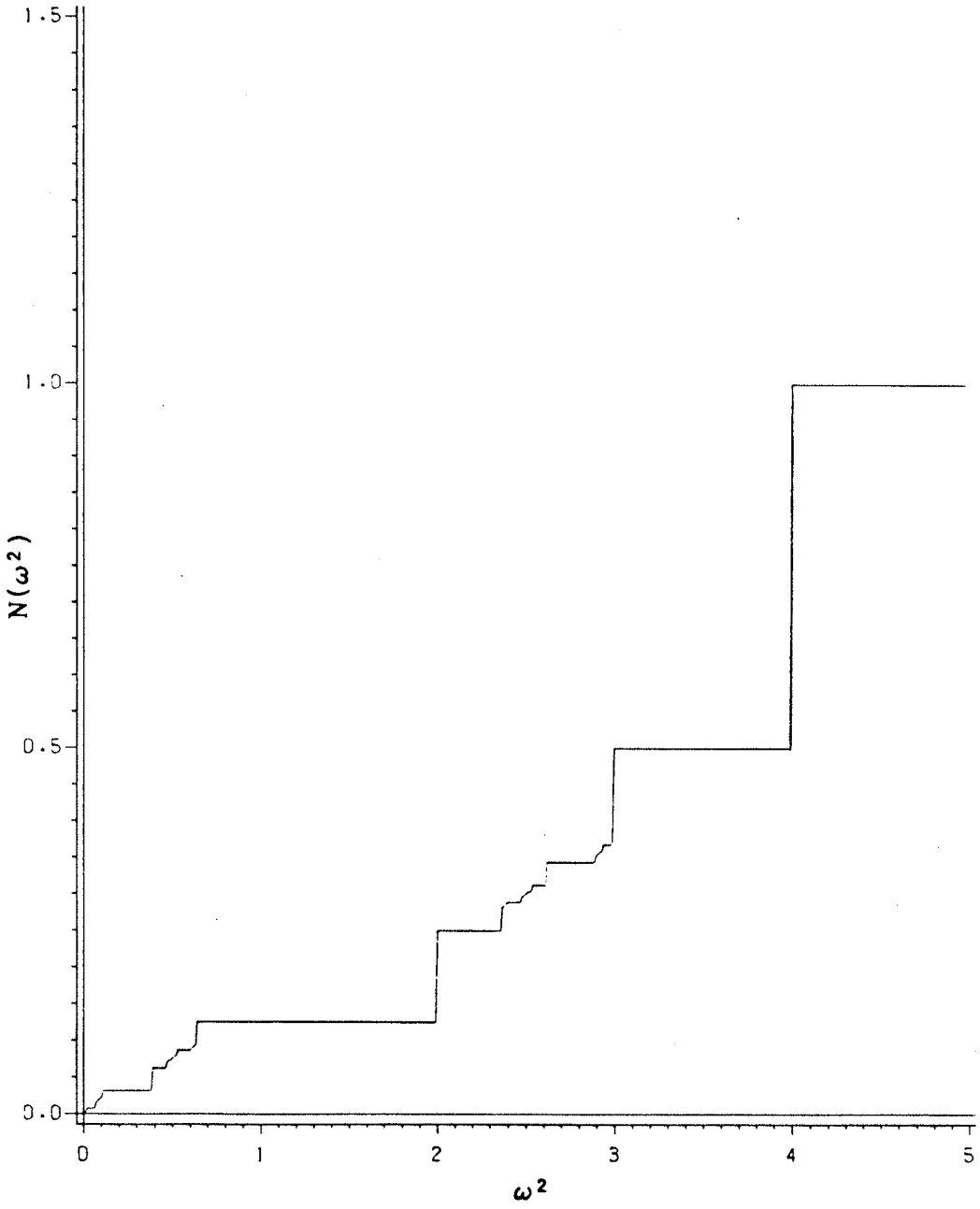

Figure 3.27: A plot of $\log(\omega_c^2)$ vs log(p-Pc) is given below. The slope of the line corresponds to the value νy=2.2 in three dimensions.

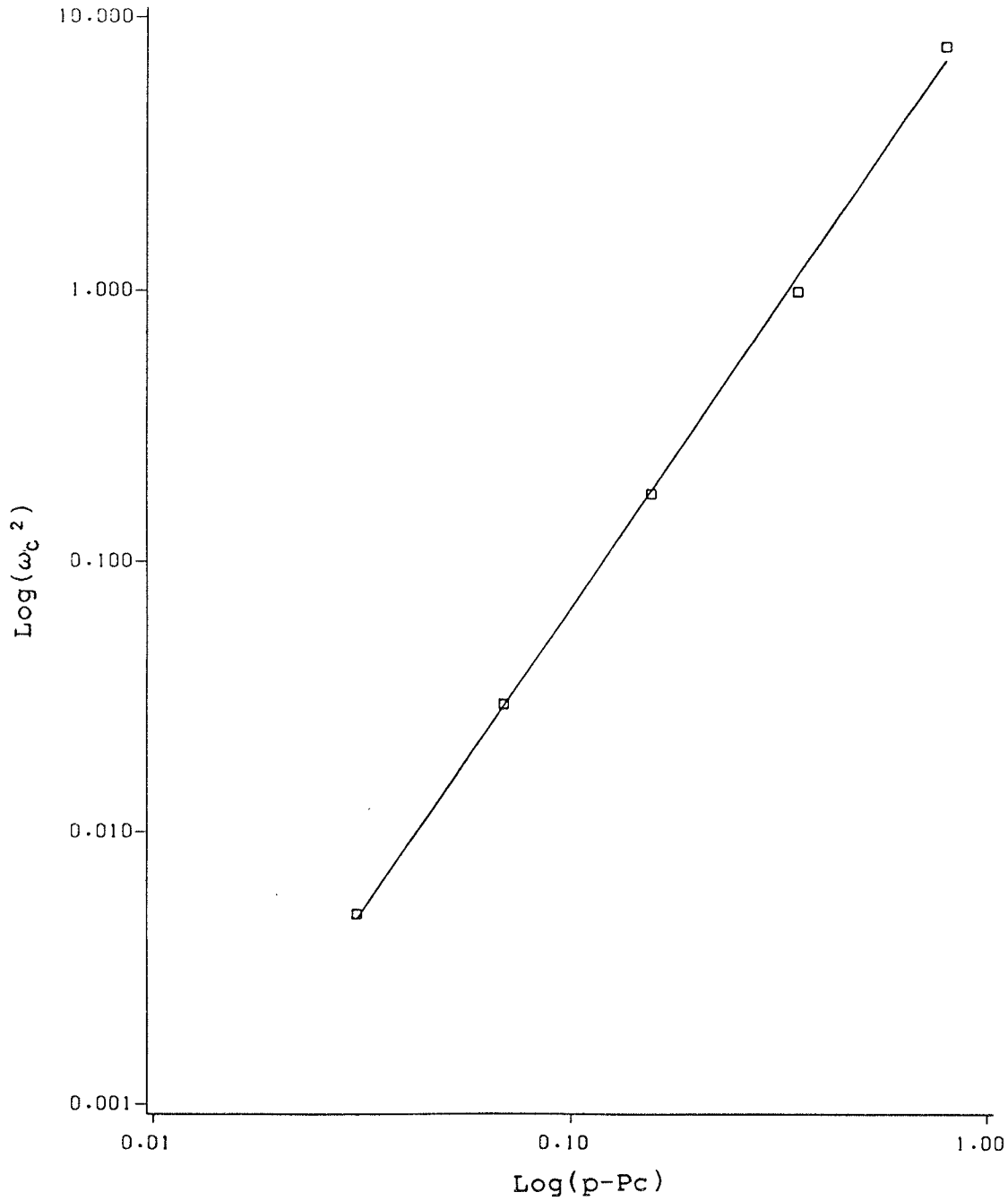

In the following section, we consider how the changes in the low frequency part of the spectrum due to the disorder affects the thermodynamic quantities such as the specific heat.

3.3 SPECIFIC HEAT

One of the thermodynamic quantities that is most useful for understanding solids is the specific heat at constant volume C_V. For both the two and three dimensional systems that we considered in sections 3.1 and 3.2, we will use the following standard expression for C_V (Ziman, 1979b)

$$C_V = k_B \int d(\omega^2)[\hbar\omega/2(k_B)T]^2[1/\sinh^2(\hbar\omega/2(k_B)T)]\rho(\omega^2) \quad [3.51]$$

where we integrate from zero frequency to some maximum value which is determined by the band edge of the density of states. For low temperatures, the behaviour is dominated by the low frequency part of the spectrum. For low values of n, this corresponds to the phonon part of the spectrum and the density of states behaves as in equation [3.34]. Using equation [3.51] above, we find the low temperature form for the specific heat to be

$$C_V \propto T^d \quad [3.52]$$

For larger values of n, the fracton part of the spectrum moves to lower frequencies. As $n \to \infty$, the density of states behaves as in equation [3.36] and the low T specific heat has the form

$$C_v \; T^{\tilde{D}} \qquad [3.53]$$

Figures 3.28 and 3.29 show our results for the specific heat of the two dimensional and three dimensional cases respectively. At low values of n, the T dependence is in accord with equation [3.52] but as n increases, we approach the behaviour of equation [3.53]. Hence there is a crossover from the expected Euclidean behaviour (T^d) to fractal behaviour ($T^{\tilde{D}}$) as a function of p-Pc. Note that there is also an increase in the specific heat at low T due to the enhancement of the density of states at low frequencies.

Figure 3.28: Below is a plot of the specific heat in two dimensions for various values of p-Pc as a function of temperature T.

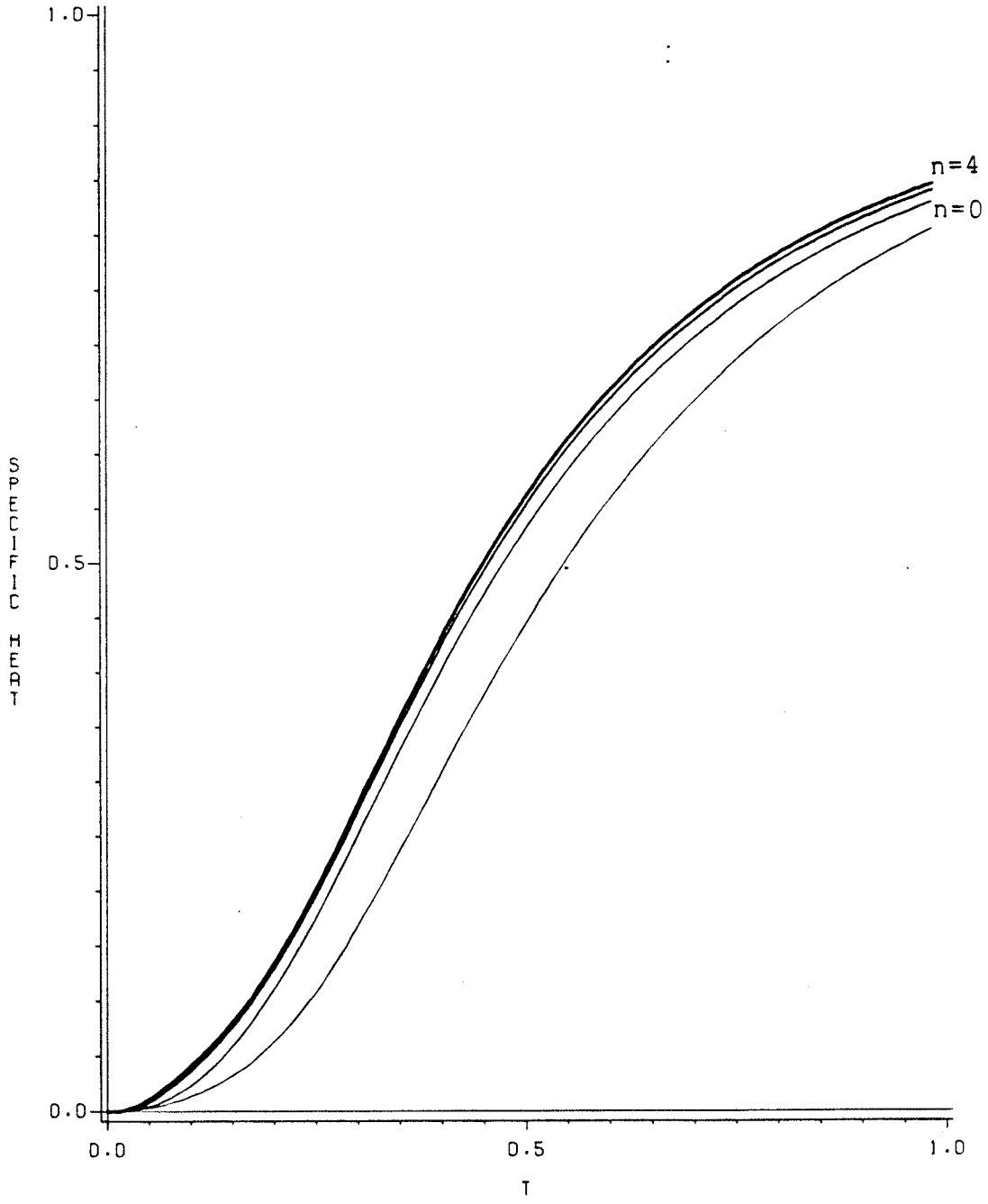

Figure 3.29: Below is a plot of the specific heat in three dimensions for various values of p-Pc as a function of temperature T.

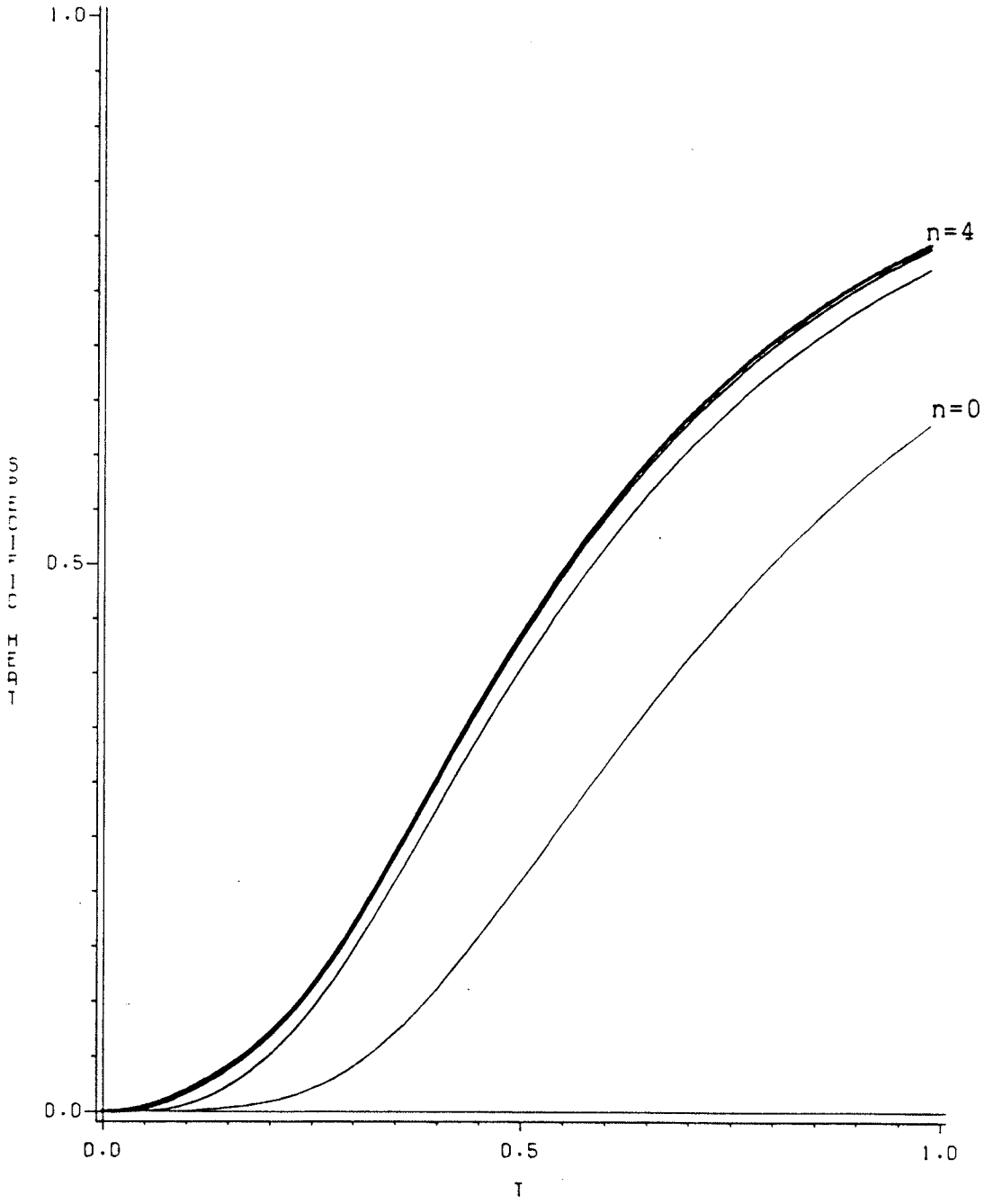

4 SUMMARY AND CONCLUSION

We have studied a model for disordered lattices and obtained the spectral properties of a TBH on these structures. The lattices are homogeneous on length scales above some distance L but are self-similar on length scales from the nearest neighour distance "a" up to L. Because the lattices lack translational invariance, conventional Fourier transform methods cannot be used. We have used a rescaling technique to calculate the spectral properties for a vibrational problem on these lattices. This technique involved using generating functions which avoided calcuating the Green's function for every site on the lattice.

Our results for the density of states clearly show that the spectrum consists of both extended and localized modes. At low frequencies, we have the phonon regime and at higher frequencies we have the fracton regime but no sharp crossover exists between regions. As we increased the amount of disorder in our lattices (increasing n), the number of continuous bands and energy gaps also increased. In fact for an infinite number of iterations, there exists an infinite number of bands and gaps. This is not surprising if we recall that the correlation length diverges in this limit and we have a disordered system with no translational invariance on any length scale.

We also found that we can characterize certain physical quantities in our systems with different dimensionalities. The density of states, for instance, is characterized by a Euclidean dimension (d) far above Pc. As we approach Pc, the low frequency behaviour changes and we require another dimension, a spectral dimension $\tilde{D}$, to describe the power-law behaviour for our fracton regime. $\tilde{D}$ is distinct from the fractal dimension D of our lattices since the fractal dimension describes only the geometrical properties.

We also considered the integrated density of states because of its smooth behaviour which made it easier to define a crossover frequency. The sudden jumps in $N(\omega^2)$ also made it easier to identify the location of the localized modes. We arbitrarily choose this frequency to be at the position of the first gap and found that, in both two and three dimensions, it decreased to zero as p-Pc approach zero. However, in contrast to the linear behaviour obtained by Derrida et al (1984), we found that the exponent has a value of 1.6 in two dimensions and 1.1 in three dimensions. We found that there was not a sudden jump between the phonon and fracton regimes at fixed p-Pc as predicted by Derrida et al (1984). Our results are supported by the recent numerical calculations of Grest and Webman (1984) who have calculated the vibrational properties of percolation clusters for a simple cubic lattice. They found that for values of p close to Pc, only a fracton regime is observed

and for p much above Pc, both phonon and fracton regimes coexist. The absence of a sharp crossover frequency between these regimes seems to be confirmed by their results.

We calculated the specific heat C_v for our disordered system and found that the behaviour at low T and for small values of ($n \leq 2$) was quite different from the behaviour for higher n. The behaviour of C_v at low temperatures was phonon-like for small n and fracton-like at higher n; the rate of increase of the specific heat at low temperatures and small values of n is smaller than that at higher values of n. These results indicate that a crossover occurs between fracton and phonon regimes as a function of p-Pc.

The models of disordered lattices presented here have something in common with some recently discovered "quasicrystals" (Levine and Steinhardt, 1984; Shechtman et al, 1984) which are crystals with quasi-periodic, rather than periodic, translational order. It is believed that materials with chemical composition Al_6Mn, have long range icosahedral orientational order. The astounding feature of these crystals is that they give diffraction patterns with sharp Bragg peaks although they do not have the translational periodicity of crystals. Until recently, it was believed that only pure crystals with translational invariance could give such diffraction patterns. Our models of disordered systems are neither random nor translationally invariant, that is, neither glassy or

crystalline. However, they do have orientational order; all triangles and tetrahedra on all scales of length have the same orientation in space. Below the correlation length, our systems are quasi periodic in that once we lay down the first triangle, the positions of the remaining triangles after subsequent iterations are determined (and not random). The real quasicrystals also exhibit self-similar properties not unlike the type we have encountered (i.e. certain patterns repeat themselves on ever larger scales as the quasi-lattices grow). It has also been reported (Levine and Steinhard, 1984) that the vibrational density of states of these quasicrystals, like our disordered systems, have a self-similar sequence of energy bands and gaps. Hence, on the basis of our results, we would expect the thermodynamic properties of these materials to exhibit non-phonon behaviour at low temperature.

APPENDIX A

In this appendix we show how the Green's functions in equation [2.41] are related to the functional integral F. Consider the following integral

$$I=\int Du\ u(1)[\delta\exp(iS)/\delta u(m)].[\int Du\ \exp(iS)]^{-1} \qquad [A.1]$$

where Du is given by equation [2.36] and

$$S=(1/2)\{\sum_i [E-\epsilon(i)]u(i)^2 - \sum_{i\neq j} V(i,j)u(i)u(j)\} \qquad [A.2]$$

Integrating the numerator by parts, it is easily shown that

$$I=-\delta(1,m) \qquad [A.3]$$

However if we compute I using

$$\delta\exp(iS)/\delta u(m)=(i)\exp(iS)\{[E-\epsilon(m)]u(m)-\sum_k V(m,k)u(k)\} \qquad [A.4]$$

then we have

$$\frac{-i\int Du\ \exp(iS)\{[E-\epsilon(m)]u(1)u(m)-\sum V(m,k)u(m)u(k)\}}{\int Du\ \exp(iS)} =\delta(1,m) \qquad [A.5]$$

If we define

$$G(1,m)=[-i\int Du\ u(1)u(m)\exp(iS)].[\int Du\ \exp(iS)]^{-1} \qquad [A.6]$$

then equation [A.5] is identical to equation [1.9]. F is thus a generating function for the Green's function equations.

BIBLIOGRAPHY

Alexander S., Orbach R., J. Physique Lett. 43, (1982), L-625

Anderson P.W., Phys. Rev., 109, (1958), p 1492

Ashcroft N., Mermin D., Solid State Physics, Holt Rinehart and Winston, (1976)

Bloch F., Z. Physik, 52, (1928), p 555

Broadbent S., Hammersley J.M., Proc. Camb. Phil. Soc., 53, (1957), p 6229

Dean P., Proc. Roy. Soc. London, A260, (1961), p 263

Dean P., Rev. Mod. Phys., 44, (1972), p 127

Derrida B., Orbach R., Kin-Wah Yu, Phys. Rev. B, 29, (1984), p 2477

Economou E.N., Green's Functions in Quantum Physics, Springer-Verlag, second edition, New York, (1983)

Essam J.W., Rep. Prog. Phys., 3, (1980), p 835

Gefen Y., Aharony A., Mandelbrot B.B., Kirkpatrick S., Phys. Rev. Lett., 27, (1981), p 1771

Grest G.S., Webman, J. Physique Lett. 45, (1984), L- 1155

Haydock R., Solid State Physics, 35, Academic Press, New York, (1980), p 215

Horiguchi T., J. Math. Phys., 13, (1972), p 1411

Levine D., Steinhardt P.J.,Phys. Rev. Let., 53, (1984), p 2477

Mandelbrot B.B., Fractals: Form, Chance and Dimension, Freeman, San Francisco, (1977)

Mandelbrot B.B., The Fractal Geometry of Nature, Freeman, San Francisco, (1979)

Morita T., Horiguchi T., J. Math. Phys., 12, (1970), p 981

Rammal R., J. Physique, 45, (1984), p 191

Rammal R., Toulouse G., J. Physique Lett. 44, (1983), L- 13

Rickayzen G., Green's Function and Condensed Matter, Academic Press, New York, (1980)

Shechtman D., Blech I., Gratias D., Cahn J.W., Phys. Rev. Lett. 53, (1984), p 1951

Southern B.W., Kumar A., Loly P.D., Tremblay A.-M.S., Phys. Rev. B, 27, (1983a), p 1405

Southern B.W., Kumar A., Ashraff J., Phys. Rev. B, 28, (1983b), p 1785

Southern B.W., Loly P.D., J. Phys. A, 18, (1985), p 525

Stauffer D., Phys. Rep., 54, (1979), p 3

Thouless D.J., Percolation and Localization, Draft of notes for lectures at Les Houches, Dept. Phys., Queen's University, Kingston, Canada, (July, 1978)

Tremblay A.-M.S., Southern B.W., J. Physique Lett., 44, (1983), L- 843

Wilson K.G., Phys. Rev B, 4, (1971a), p 3174

Wilson K.G., Phys. Rev B, 4, (1971b), p 3184

Zallen R., The Physics of Amorphous Solids, Wiley, New York, (1983)

Ziman J.M., Models of Disorder, Cambridge, (1979a)

Ziman J.M., Principles of the Theory of Solids, second edition, Cambridge, (1979b)